

AMERICAN UNIVERSITY OF BEIRUT

DRAINED INTERFACE STRENGTH BETWEEN PIPELINES
AND CLAYS USING TILT TABLE AND DIRECT SHEAR
TESTS

by
RAYAN BOU MJAHEB

A thesis
submitted in partial fulfillment of the requirements
for the degree of Master of Engineering
to the Department of Civil and Environmental Engineering
of the Maroun Semaan Faculty of Engineering and Architecture
at the American University of Beirut

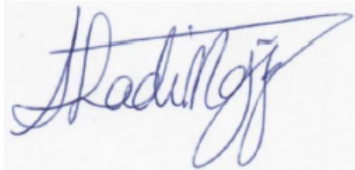
Beirut, Lebanon
July 2020

AMERICAN UNIVERSITY OF BEIRUT

DRAINED INTERFACE STRENGTH BETWEEN PIPELINES
AND CLAYS USING TILT TABLE AND DIRECT SHEAR
TESTS

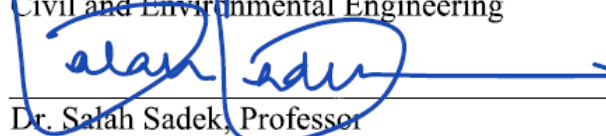
by
RAYAN BOU MJAHEB

Approved by:



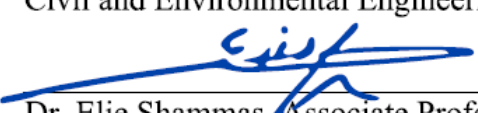
Dr. Shadi Najjar, Associate Professor
Civil and Environmental Engineering

Advisor



Dr. Salah Sadek, Professor
Civil and Environmental Engineering

Co-Advisor



Dr. Elie Shammas, Associate Professor
Mechanical Engineering

Committee member

Date of thesis defense: June 19, 2020

AMERICAN UNIVERSITY OF BEIRUT

THESIS, DISSERTATION, PROJECT RELEASE FORM

Student Name: Bou Mjahed Rayan Akram
Last First Middle

Master's Thesis Master's Project Doctoral Dissertation

I authorize the American University of Beirut to: (a) reproduce hard or electronic copies of my thesis, dissertation, or project; (b) include such copies in the archives and digital repositories of the University; and (c) make freely available such copies to third parties for research or educational purposes.

I authorize the American University of Beirut, to: (a) reproduce hard or electronic copies of it; (b) include such copies in the archives and digital repositories of the University; and (c) make freely available such copies to third parties for research or educational purposes

after: **One --- year from the date of submission of my thesis, dissertation, or project.**

Two --- years from the date of submission of my thesis, dissertation, or project.

Three -- years from the date of submission of my thesis, dissertation, or project.



July 08, 2020

Signature

Date

ACKNOWLEDGMENTS

I would like to express my gratitude to my advisors Dr. Shadi Najjar and Dr. Salah Sadek for their valuable, unbounded, and unlimited technical, theoretical, and academic assistance throughout the different stages of my thesis work. I would also like to thank Dr. Elie Shamma for serving on my committee and reviewing my thesis.

The simple and efficient technical ideas provided by Mr. Helmi Al-Khatib and Miss Dima Al Hassanieh were extremely helpful. Truly, I express my deep gratitude and thankfulness to them. Special thanks are extended to Mrs. Zakia Deeb for her administrative assistance.

Finally, I want to thank my family for their full support and commitment to make this journey possible.

AN ABSTRACT OF THE THESIS OF

Rayan Bou Mjahed for Master of Engineering
Major: Civil Engineering

Title: Drained Interface Strength between Pipelines and Clays Using Tilt Table and Direct Shear Tests

The design of high-pressure high-temperature pipelines (HPHT pipelines) is mainly governed by pipe-soil interaction considerations. Over the past few years, a number of studies have set as their goal to reliably characterize the soil-pipeline interface behavior. Independent research groups utilized different test setups and methodologies to that effect, with the tilt table test and the interface direct shear test being the most common testing approaches. To date, there are no published efforts that show direct comparisons between results from these two testing systems. The objectives of this study are to (1) design and fabricate tilt table and interface direct shear testing setups that are capable of measuring the drained interface resistance between pipelines and clays, (2) use these setups to study the effects of low effective normal stresses and type of pipeline coating on the drained clay-pipe interface response, and (3) compare the results from tilt table and interface direct shear tests under identical interface and soil conditions. The results allow for drawing conclusions on the adequacy of the two testing methodologies in determining interface strength properties that will aid the design of offshore pipelines in soft clays.

CONTENTS

ACKNOWLEDGEMENTS.....	V
ABSTRACT.....	VI
LIST OF ILLUSTRATIONS.....	IX
LIST OF TABLES.....	XV
Chapter	
1. INTRODUCTION.....	1
2. LITERATURE REVIEW	3
2.1.Laboratory element testing	3
2.2.Laboratory model testing.....	10
2.3.In-situ testing	18
2.4.Pipe-Soil Interaction Framework.....	22
3. TESTING MATERIALS	24
3.1.Soils	24
3.2.Interfaces.....	26
4. INTERFACE DIRECT SHEAR TESTING.....	28
4.1.Modified Direct Shear Apparatus.....	28

4.2. Testing procedure (sample preparation, consolidation, and shearing phase).	30
4.3. Important considerations to minimize friction for direct shear testing at low normal stresses:	32
4.4. Measurement of the horizontal and vertical friction.	36
5. TILT TABLE TESTING	39
5.1. Tilt Table Apparatus.	39
5.2. Testing Procedure.	40
5.3. Important considerations for tilt table testing:	43
6. TESTING CONCEPT	45
7. EXPERIMENTAL RESULTS AND DISCUSSION	46
7.1. Consolidation response.	46
7.2. Peak and residual interface resistances from the Interface Direct Shear tests...	51
7.3. Residual interface resistance from tilt table tests.	62
7.4. Effect of roughness.	66
7.5. Comparison between the two testing methodologies.	68
7. CONCLUSION	71
REFERENCES	73

ILLUSTRATIONS

Figure	Page
1 - Tilt table frame and sliding of the plate at failure	3
2 - (a) Modified direct interface shear box devices, and (b) a schematic illustration of the test setup.....	5
3 - Schematic diagram of the Cam-shear shear box showing the main features and photograph of Cam-shear test setup.....	6
4 - Plots of "fast" shear test (0.5mm/s) showing interface strength plotted against shearing displacement. Upper test data: rough interface; lower test data: smooth interface.	7
5 - Comparison of rough interface strength profiles when shearing at slow (0.001mm/s) and fast (0.5mm/s) speeds.....	8
6 - General view of ring shear apparatus showing components utilized to apply low normal stresses and measure corresponding shear forces. LVDT, linear variable differential transducer.	9
7 - Photograph and Schematic diagram of the Cam-Tor machine.....	9
8 - Connection of load cell between the test and end sections	11
9 - Pipe and end sections.....	11
10 - Initial embedment of the pipe.....	11
11 - Schematic of loading rig.....	12
12 - Measured axial pulling force during the 13 sweeps	12

13 - Schematic diagram of the macro-scale interface direct shear test device and test setup.....	14
14 - Photograph of the macro-scale interface direct shear test device.....	14
15 - Photograph illustrating the hinged connection between the load cell and the threaded rod transferring the tensile force to the mobile frame (note that the hinge shown is in a state with no load applied, hence the slack at the hinge in the diagram)..	15
16 - Test arrangement showing clearance of soil at pipe ends.	16
17 - Assembled model pipe, S-shaped axial load cell and loading arm	16
18 - Photograph of end of model pipe in test trough, showing pulling arrangement (University of Cambridge).....	17
19 - Schematic diagram of the axial model testing (University of Cambridge).....	18
20 - Schematic of ROV-based drag test concept.	19
21 - Free body diagram of tool during testing.	20
22 - Schematic view of Smartpipe tool.....	21
23 - Cutaway view of model pipe and pore pressure transducers on pipe surface	21
24 - Axial pipe-soil interaction framework.....	22
25 - Schematic for axial resistance displacement response	23
26. Particle-size distribution of the Natural Clay	25
27. Particle-size distribution of the High Plasticity Clay	26
28. Particle-size distribution of the Kaolinite	26
29. 90x60 mm size Stainless Steel interface fitted into the lower shear box of the interface direct shear.....	27
30. Sandpaper glued to a plastic sheet for Tilt Table testing.....	27
31. Modified Direct Shear Machine (Modified components).....	29

32. Custom-fabricated Teflon shear box.....	29
33. LabVIEW code	29
34. Data acquisition system placed inside the electronic box.....	30
35. Sample preparation.	31
36. Tape attaching the interface tightly to the lower shear box.....	33
37. Filter paper trimmed to the size of the shear box.	34
38. Porous stone trimmed.	34
39. Spreading of oil on to minimize friction.....	35
40. Smaller area of loading gap, and screw nut used to connect the upper shear box and the load cell.....	36
41. Vertical measurement setup.....	37
42. Vertical measurement setup closer view.	37
43. Comparison between interface friction angle with and without correction for vertical and horizontal friction.....	38
44. Tilt table testing setup.....	39
45. Spreading of the 2mm specimen on the interface.....	40
46. First phase of consolidation under loading plate only.	40
47. Tilt table setup placed inside the Plexi water bath.....	41
48. Tilt table setup as is inside the water bath.	42
Figure 49. Slipping phase on the tilt table.	43
50. Tilt Table Apparatus	Error! Bookmark not defined.
51. Consolidation of Natural Clay - Plexiglass (10mm thick specimen)	46
52. Consolidation of Natural Clay - Stainless Steel (10mm thick specimen).....	47
53: Consolidation of Natural Clay - Sandpaper (10mm thick specimen).....	47

54. Consolidation of High Plasticity Clay - Stainless Steel (10mm thick specimen).....	48
55. Consolidation of High Plasticity Clay - Sandpaper (10mm thick specimen).....	48
56. Consolidation of Kaolinite - Stainless Steel (10mm thick specimen)	49
57. Consolidation of Kaolinite - Stainless Steel (10mm thick specimen)	49
58. Consolidation of the Natural Clay (20mm thick specimen)	50
59. Consolidation of the High Plasticity Clay (20mm thick specimen)	50
60. Consolidation of the Kaolinite (20mm thick specimen).....	51
61. Failure mechanism of HPC on the Stainless Steel.....	52
62. Failure mechanism of HPC on the Sandpaper.....	53
63. Direct shear test on the Kaolinite.....	53
64. Interface direct shear results of NC-Plexiglass interface (a) shear stress vs displacement, (b) failure envelopes, (c) settlement during shearing, and (d) secant friction angles.	54
65. Interface direct shear results of NC-Steel interface (a) shear stress vs displacement, (b) failure envelopes, (c) settlement during shearing, and (d) secant friction angles.	55
66. Interface direct shear results of NC-Sandpaper interface (a) shear stress vs displacement, (b) failure envelopes, (c) settlement during shearing, and (d) secant friction angles.	56
67. Interface direct shear results of HPC-Steel interface (a) shear stress vs displacement, (b) failure envelopes, (c) settlement during shearing, and (d) secant friction angles.	57
68. Interface direct shear results of HPC-Sandpaper interface (a) shear stress vs displacement, (b) failure envelopes, (c) settlement during shearing, and (d) secant friction angles.	58

69. Direct shear tests results of the Kaolinite, and the Kaolinite on the Stainless Steel and Sandpaper: (a) shear stress vs displacement, (b) secant friction angles, and (c) settlement during shearing.	59
70. Direct shear tests results of NC at low normal stress (a) shear stress vs displacement, (b) failure envelopes, (c) settlement during shearing, and (d) secant friction angles.	60
71. Direct shear tests results of HPC at low normal stress (a) shear stress vs displacement, (b) failure envelopes, (c) settlement during shearing, and (d) secant friction angles.	61
72. Failure mechanism of the natural clay on: (a) the Stainless Steel and (b) the Sandpaper.....	62
73. Variation of (a) peak interface strength and (b) peak secant friction angle with normal stresses using the tilt table (for the NC)	63
74. Variation of (a) residual interface strength and (b) residual secant friction angle with normal stresses using the tilt table (for the NC)	63
75. Variation of (a) peak interface strength and (b) peak secant friction angle with normal stresses using the tilt table (for the HPC)	64
76. Variation of (a) residual interface strength and (b) residual secant friction angle with normal stresses using the tilt table (for the HPC)	64
77. Variation of (a) peak interface strength and (b) peak secant friction angle with normal stresses using the tilt table (for the KAO)	65
78. Variation of (a) residual interface strength and (b) residual secant friction angle with normal stresses using the tilt table (for the KAO)	65
79. The variation of the drained strength ratio with the roughness on the interface direct shear testing setup.....	66

80. The variation of the interface efficiency with normal stresses on the tilt table testing setup.....	67
81. Residual friction angles for: (a) Plexiglass, (b) Steel and (c) Sandpaper from Tilt table and direct shear results (for the Natural Clay).....	69
82. Residual friction angles for: (a) Steel and (b) Sandpaper from Tilt table and direct shear results (for the High Plasticity Clay).....	70
83. Residual friction angles for: (a) Steel and (b) Sandpaper from Tilt table and direct shear results (for the Kaolinite)	70

TABLES

Table	Page
1. Soils Characteristics.....	24
2: Stand time for reconstituted sample as per ASTM D3080 section 7.2.....	25
3. Difference between theoretical and actual measured normal stress.	37

CHAPTER 1

INTRODUCTION

The design of high-pressure and high-temperature pipelines (HPHT pipelines) is mainly governed by the pipe-soil interaction. Many researchers have tried to quantify the key parameters of the axial pipe-soil resistance using laboratory element testing apparatuses like the tilt table (Najjar et al. 2003, 2007; Pedersen et al. 2003), the interface direct shear (Boukpeti and White 2017; Hill et al. 2012; Low et al. 2017; Randolph et al. 2012; Westgate et al. 2018; White et al. 2012), the cam-shear (Ganesan et al. 2014; Haustermans 2002) and few types of modified torsional shear devices (Eid et al. 2014; Kuo et al. 2015).

On another front, several efforts have targeted measuring the axial pipe-soil resistance in-situ. In-situ field testing is expected to result in more accurate interface results, eliminating the need for sampling soils, sending them to the laboratory, and preparing them for testing. Such in-situ testing tools are very few, the most important of which is the Fugro SMARTPIPE testing system which is associated with relatively high testing costs and complicated testing methodologies.

The two most common laboratory testing approaches for measuring the interface strength between pipelines and clays are the tilt table test and the interface direct shear test. The tilt table device relies on gravity loading and allows for the reproduction of low confinement test conditions and relatively large displacements resulting in reliable measurement of the drained residual interface shear resistance. On the other hand, interface direct shear devices are usually custom-fabricated and

modified to allow for reliable testing at low confining pressure and repeated cycles/reversals are needed to allow for the mobilization of residual conditions.

Till date, there are no published efforts that show direct comparisons between results from these two testing systems. Thus, the objective of the proposed research is to design and fabricate tilt table and interface direct shear testing setups that are capable of measuring the drained interface resistance between pipelines and clays and use these setups to study the effects of low effective normal stresses, type of pipeline coating, and soil composition on the drained peak and residual clay-pipe interface response. The ultimate goal of this series of tests is to compare the results from tilt table and interface direct shear tests under identical interface and soil conditions and provide recommendations on the use and value of these two test alternatives. In what follows is a comprehensive literature review that targets the different efforts that were aimed at measuring the pipe-soil interaction.

CHAPTER 2

LITERATURE REVIEW

2.1. Laboratory element testing

Conventional geotechnical test setups are not designed to perform tests under low effective normal stresses. New setups have been invented and few have been modified to make them capable of shearing a soil sample on a pipe coating interface, while accounting for the low normal stress range.

Najjar et al. (2003, 2007) and Pedersen et al. (2003) presented test results that were performed on a tilt table device (Figure 1) to measure the drained residual shear strength mobilized at the interface between several pipeline coatings and fine-grained soils. The tilt table is a simple device that uses gravity to apply normal and shear stress, eliminating the friction errors resulting from mechanical systems.

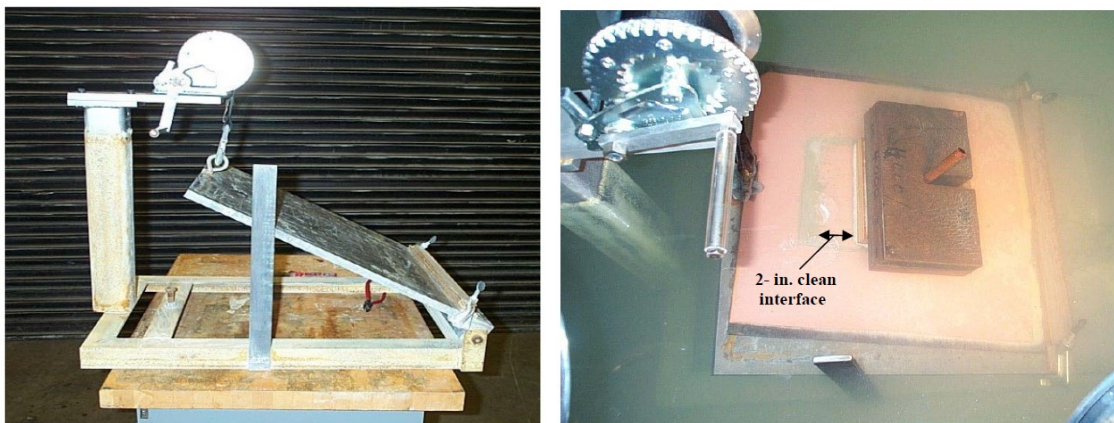


Figure 1 - Tilt table frame and sliding of the plate at failure

Najjar et al. (2007) measured the drained residual strength of the clay-clay and clay-coating interface at effective normal stresses ranging between 1.7 and 5.8 kPa. For the tests that aimed at measuring the residual interface shear strength, the thickness of

the soil specimen was 1.5mm, whereas for the ones that measure the internal residual shear strength of the clay, the thickness was 2.5mm. The rate of shearing was slow enough to allow dissipation of water and ensure drained conditions, with the time to failure taken as $t_f = 50t_{50}$. The tilt table device allows for large shearing displacement depending on its size. The residual shear strength was reached after a displacement of 25-50 mm, with recorded interface friction of 20° for the highest effective stress used (5.8 kPa) and 32° for the lowest (1.7 kPa). The interfaces roughness was less than $50\mu\text{m}$, and coating efficiency – defined as the interface residual strength with respect to residual strength of soil – ranged between 60% and 90%. A total of 54 tests led to the conclusion that the type of coating and composition of soil are the factors that affect the residual shear strength at the pipe-soil interface.

Another common test method that is used to quantify axial pipe-soil resistance is the Interface Shear Box (ISB) test. The published work that have adopted the latter in recent years includes Boukpeti and White (2017), Hill et al. (2012), Low et al. (2017), Randolph et al. (2012), Westgate et al. (2018) and White et al. (2012). The device is basically a conventional direct shear box, but with the bottom part replaced by an interface material that is sheared against a top part containing the soil specimen. Applying low effective normal stresses should not be through the conventional lever arm of the direct shear because of the uncertainty and significant friction that accompany its use at low normal stresses. Figure 2 shows the modified interface direct shear devices built by testing equipment companies like Humboldt and Geocomp.

Boukpeti and White (2017) presented interface test results for two marine clays studying the effect of undrained and partially drained shearing, and consolidation during and in-between shearing cycles on the axial pipe-soil resistance. In this study, a rough

and smooth interface of $R_a > 80 \mu\text{m}$ and $R_a \approx 2 \mu\text{m}$ respectively were used. Westgate et al. (2018) collected data constituting more than 200 tests performed on several soft clays and pipeline coatings and suggested a site-specific test program using the ISB device in order to get initial estimate of the axial pipe-soil interaction parameters. The tests have been performed under effective normal stresses that range between 2 to 14 kPa and using shearing rates between 0.001mm/s and 0.1mm/s while performing cycles of shearing in both directions. The testing device is gaining more popularity, but careful attention must be paid to the mechanical friction of the system as its impact on the low effective stresses is important. Other limitations of the ISB testing device are its relatively short horizontal displacement and its inability to measure pore pressures developed in the soil sample.

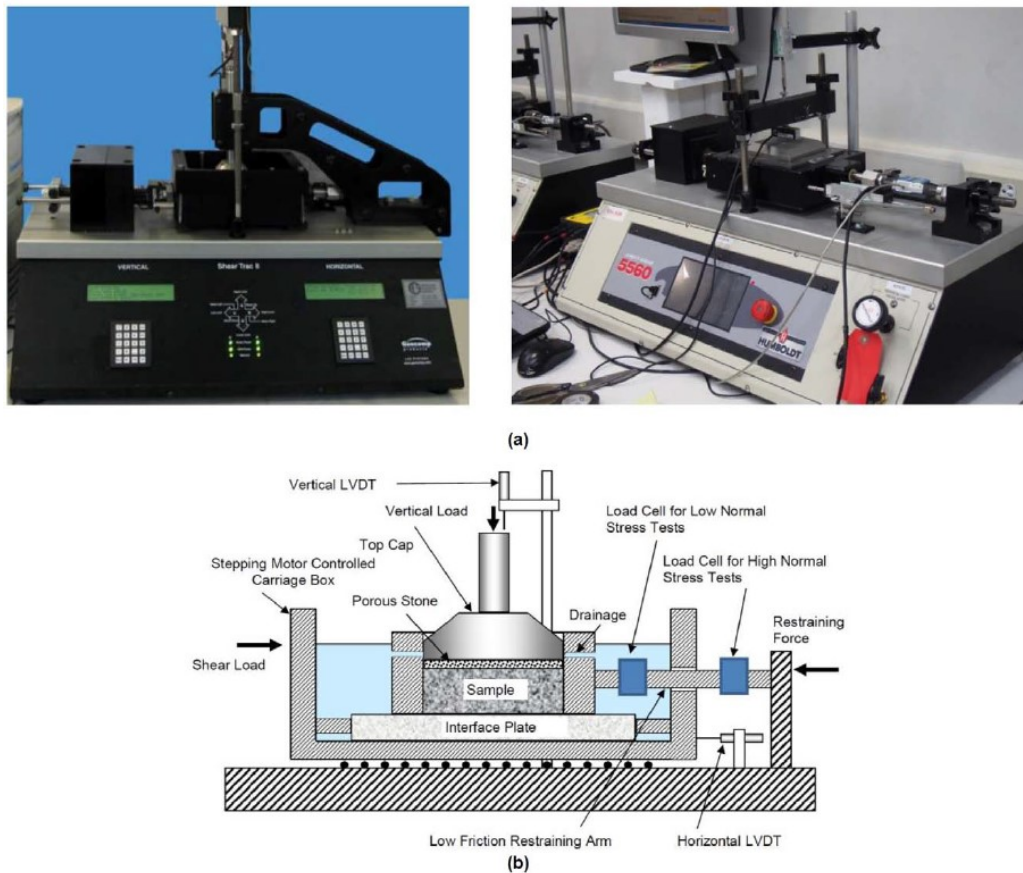


Figure 2 - (a) Modified direct interface shear box devices, and (b) a schematic illustration of the test setup.

Senthil Ganesan, Kuo, and Bolton (2014) presented a series of soil-interface and soil-soil tests performed on the Cam-Shear device (Figure 3), which is basically similar in concept to a direct shear test but with the possibility for shearing to larger displacements (reaching 190mm). The device was first introduced by Dunlop et al. (2000) and then modified by Haustermans (2002) to allow the simulation of axial pipe–soil interaction behavior.

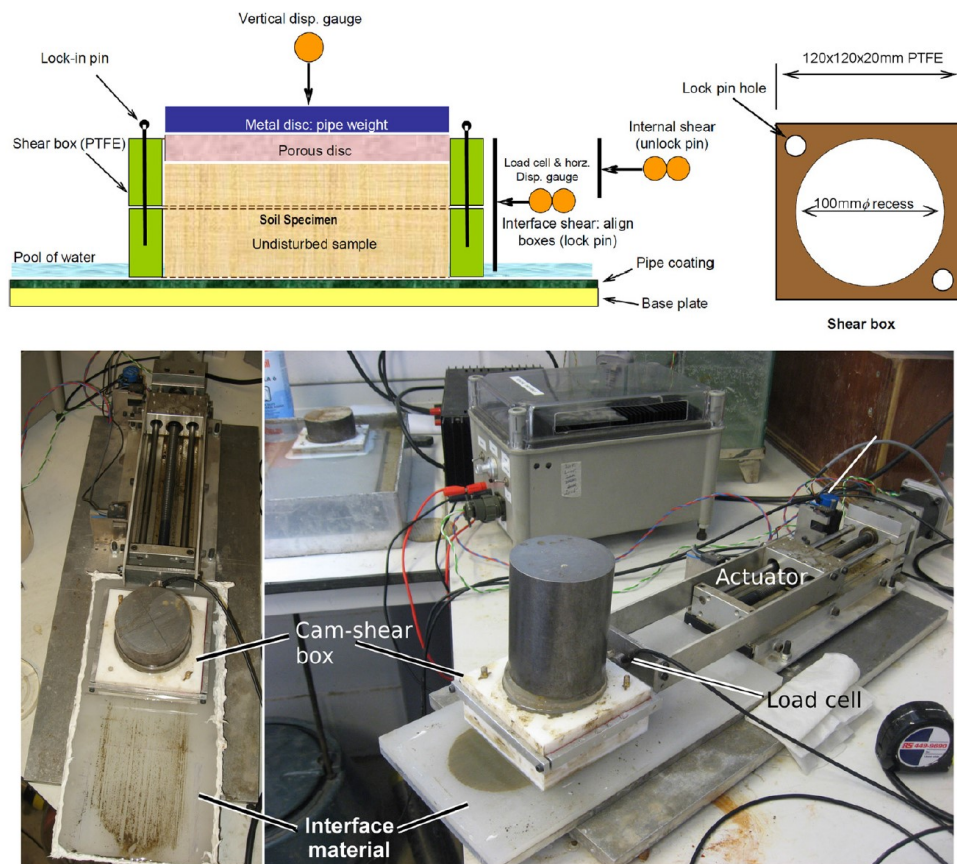


Figure 3 - Schematic diagram of the Cam-shear shear box showing the main features and photograph of Cam-shear test setup.

In the study of Senthil Ganesan et al. (2014), the shear box was made of polytetrafluoroethylene (PTFE) to minimize the inherent friction in the system. The apparatus can accommodate natural samples taken from core tubes, but the tests presented in their paper were conducted on reconstituted soft marine clays from west coast of Africa. The tested clay samples were overconsolidated under effective stresses

between 8 and 14 kPa in order to reach undrained shear strengths found in situ, and then sheared under normal stresses between 1 and 4.5 kPa. The tests were done in undrained, partially drained and drained conditions, using a shearing rate between 0.001mm/s and 0.5mm/s. The smooth and the rough interfaces material had an average surface roughness $R_a = 1.64 \mu\text{m}$ and $R_a = 67.44 \mu\text{m}$ respectively.

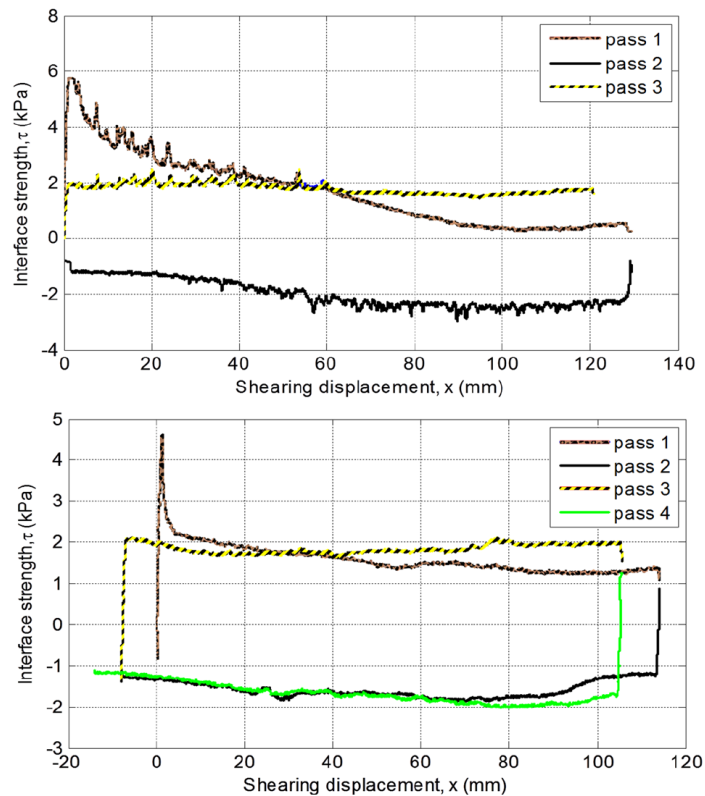


Figure 4 - Plots of "fast" shear test (0.5mm/s) showing interface strength plotted against shearing displacement. Upper test data: rough interface; lower test data: smooth interface.

Figure 4 presented sample results for the tests performed on smooth and rough interfaces at a shearing rate of 0.5mm/s. The graphs show that in the case of rough interface, there is an initial peak resistance of 5.8 kPa and then a gradual drop close to zero after shearing of 10mm, before leveling of the residual resistance to 2 kPa in the following two passes. In the case of the smooth interface, the resistance rapidly drops to

50% after 5mm and remains relatively constant. Figure 5 also presents comparison between results of tests sheared at 0.001mm/s and 0.5mm/s on a rough interface. The slow test exhibits an initial peak resistance before dropping to a constant value, whereas the fast test exhibits higher peak resistance (overconsolidated clay) before dropping gradually and more significantly than the slow test.

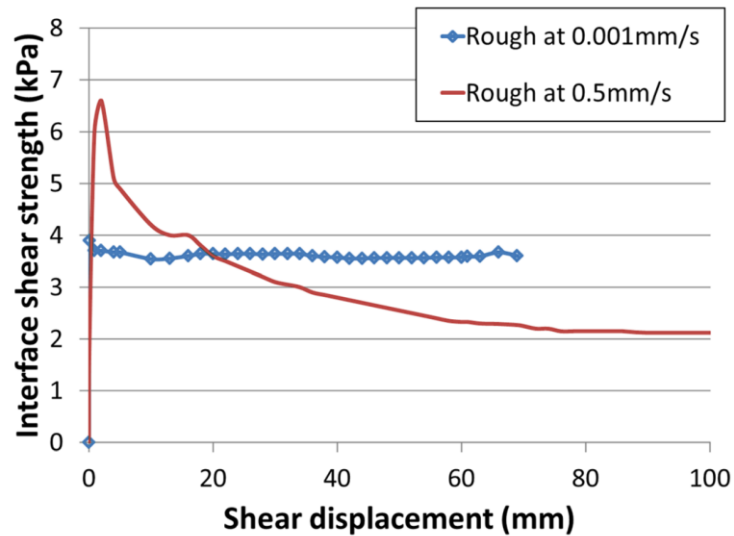


Figure 5 - Comparison of rough interface strength profiles when shearing at slow (0.001mm/s) and fast (0.5mm/s) speeds.

Modified torsional ring shear apparatuses have also been used for determination of the pipe-soil interface resistance as it permits unlimited shear displacements. Eid et al. (2014) modified a Bromhead type torsional shear device to run tests under low effective stress (3-7 kPa). Figure 6 shows that the lever system was replaced by a light weight loading assembly, the dial gauges were replaced by ones with lower capacity reading and higher accuracy, in addition to modifications done to the specimen container to accept the soil-solid shearing. In addition, changes were made in compliance with the recommendations in Stark and Eid (1993) to reduce the side-wall friction of the container. Kuo et al. (2015) and De Brier, Ballard, and Colliard (2016) presented results of tests conducted on a new torsional shear device referred to as the

The Cam-Tor (figure 7). The device was developed at University of Cambridge in collaboration with BP and Fugro and can perform tests under 2-50 kPa and at shearing rates between 0.0005 mm/s and 0.1 mm/s. The device contains a fixed circular interface with a circular soil specimen rotating above it. However, the limitation of the ring shear tests is that they exhibit variation in strain rate radially across the soil specimen.

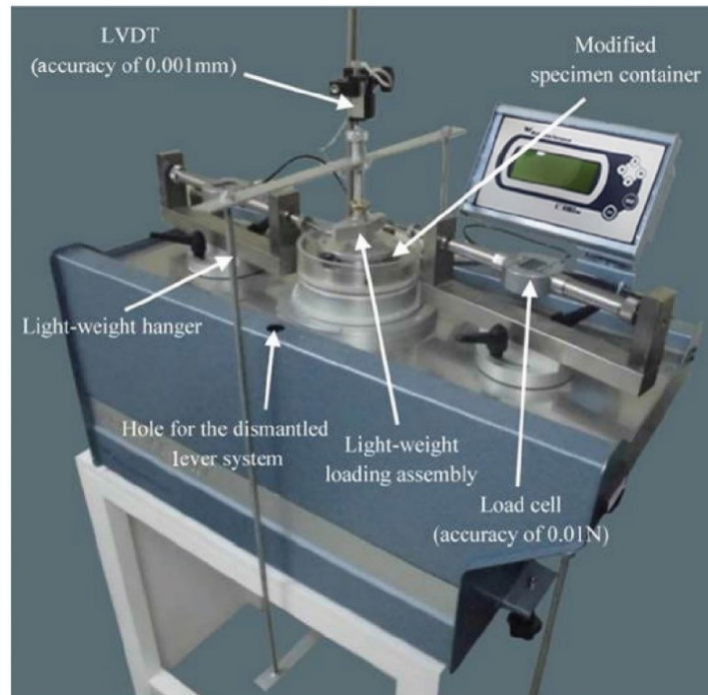


Figure 6 - General view of ring shear apparatus showing components utilized to apply low normal stresses and measure corresponding shear forces. LVDT, linear variable differential transducer.

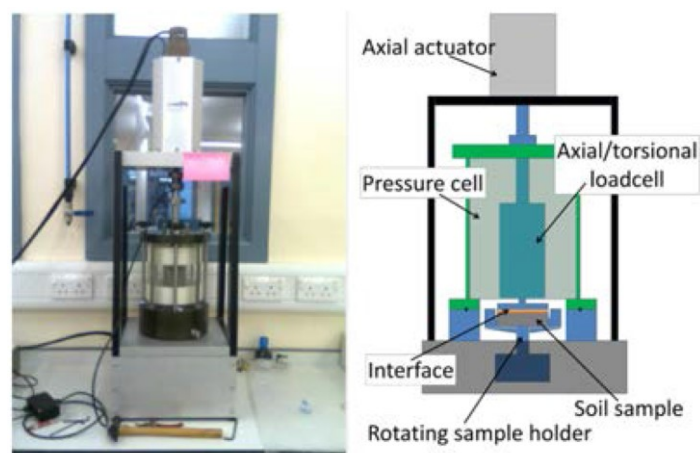


Figure 7 - Photograph and Schematic diagram of the Cam-Tor machine

2.2. Laboratory model testing

Researchers have also studied the axial pipe-soil resistance by building model test setups that mimic field condition. Senthilkumar et al. (2011) and Senthilkumar et al. (2013) designed a laboratory test setup in Monash University (Australia), named Monash Advance Pipe testing System (MAPS). The model measured the axial resistance of the interface between a steel pipe and Prestige NY kaolin. The soil bed was about 650mm thick with 450mm of kaolin overlying a 200mm draining layer of sand and separated by a 3mm geotextile membrane. The pipe is actuated vertically and horizontally at displacement rates between 0.01mm/s and 0.5mm/s and is comprised of three sections: the two end sections are dummy sections (2x175mm long), and the middle pipe section (350mm long) is connected to the end parts by S-type load cells only. In this way, the undrained and drained axial friction that acts on the middle section is measured by recording the difference between the two load cells, and the dummy sections have the purpose of eliminating the significant effect of the passive soil that acts on the embedded pipe while moving it horizontally. The pipe was displaced in a series of horizontal sweeps reaching 10mm in both directions away from its original position. Lastly, the model has a couple of limitations: First the dummy part will have already sheared the soil underneath it during horizontal movement before the arrival of the middle section into the dummy sections' location. Second, the pipe is not allowed to consolidate under its own weight during shearing, and the pipe's embedment is predetermined.



Figure 9 - Pipe and end sections



Figure 8 - Connection of load cell between the test and end sections

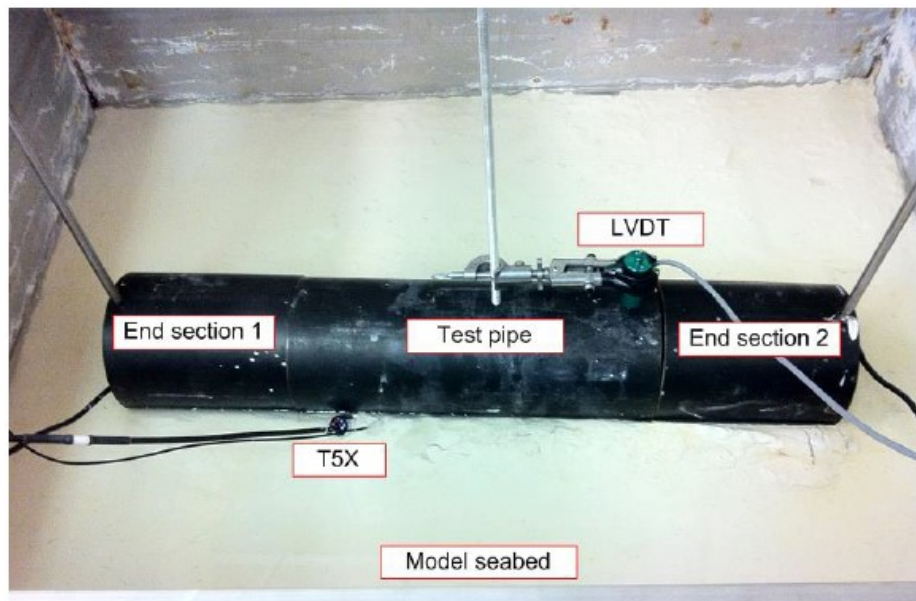


Figure 10 - Initial embedment of the pipe

At the Norwegian Geotechnical Institute (NGI) in Oslo, Smith and White (2014) studied the effect of the hardening of soil surrounding the pipe on the axial interface resistance during cycles of shearing. The test consisted of sweeping a model pipe of 1.4m in length and 120mm in diameter on a reconstituted glaciomarine clay in a 3.4x1.75m bed. The tests were performed under an effective normal stress of 5.4 kPa. The pipe was penetrated initially to a depth of 0.3D and was then moved 150mm axially in each sweep at a displacement rate of 0.01mm/s. The pipe was polypropylene coated and sand blasted with an average surface roughness R_a of 21 μ m. 13 pore pressure

transducers were placed at the bottom of the pipe to measure the excess pore pressures generated throughout the test. To remove the additional soil resistance due to end effects, the soil was scraped away manually from the ends of the pipe.

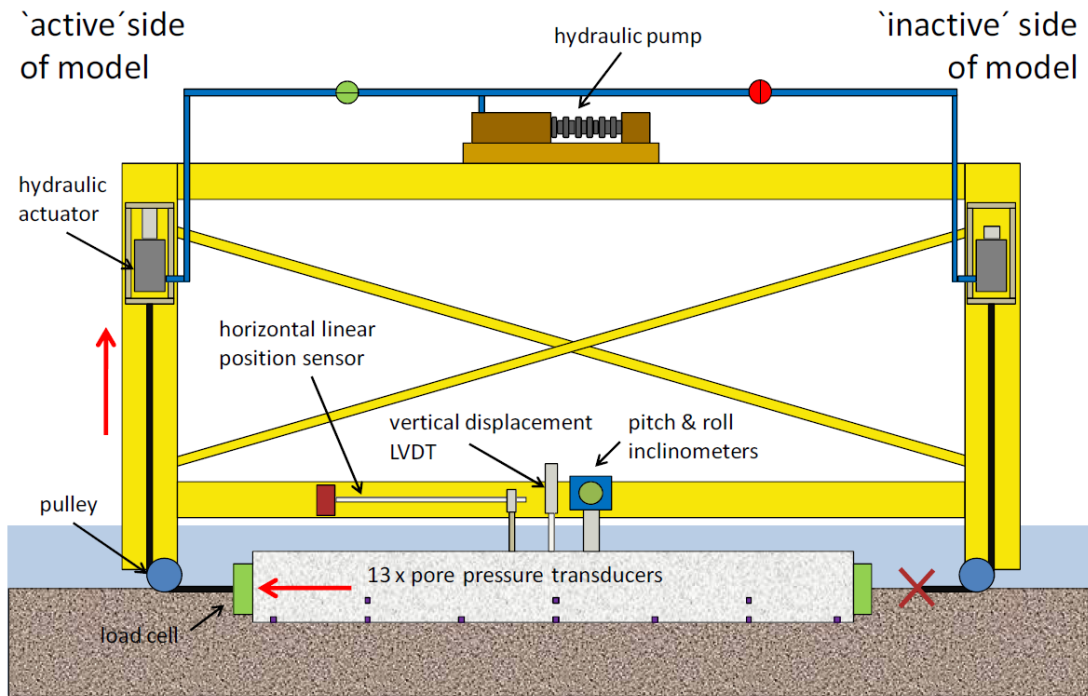


Figure 11 - Schematic of loading rig

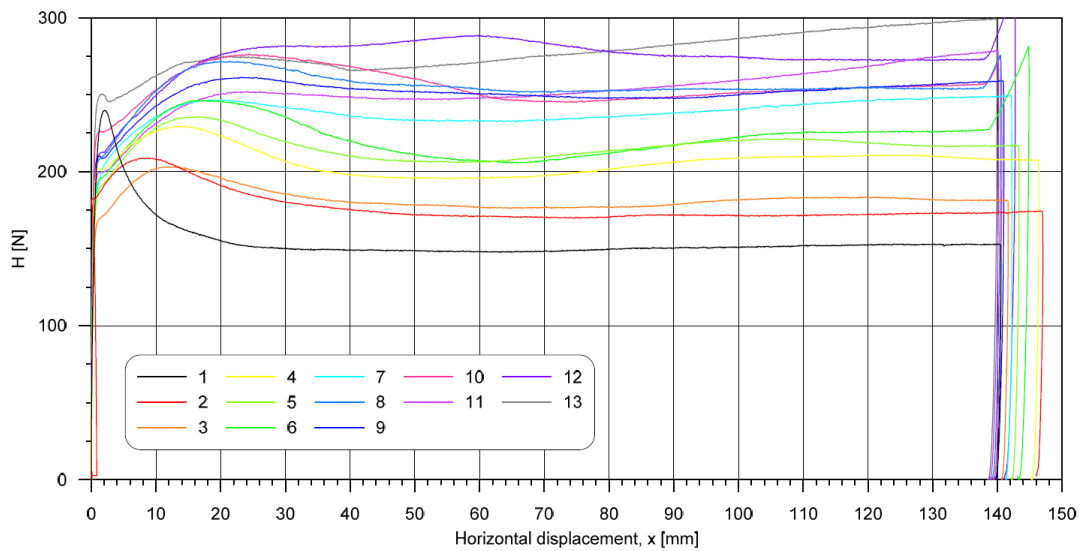


Figure 12 - Measured axial pulling force during the 13 sweeps

In the above graph, the numbers refer to the number of sweeps. The first sweep shows an initial brittle peak in resistance, and with each sweep there is an increase in the residual axial resistance. This increase is explained by a volumetric hardening of the soil underneath the pipe, thus an increase in the undrained shear strength of the soil. The authors note that only one shearing rate was used and shearing at higher rate was not explored.

Wijewickreme, Amarasinghe, and Eid (2014) developed a macro-scale interface direct shear apparatus for determining the soil-solid drained shear strength at large displacement and under low effective normal stresses. The device is similar in concept to the conventional small-scale direct shear box but with the advantage of a larger interface shear area of 3m^2 ($1.72 \times 1.75\text{m}$), and a large achievable shearing displacement of 1.2m (figure 13). The shear displacement rates that were used in the study range from 0.0001mm/s to 1mm/s depending on the type of soil in use. The apparatus also comprises of 7 pore water pressure transducers mounted flush with the interface material in order to measure the excess pore water pressures and accurately determine the effective normal stresses. The study presents results of tests performed on Fraser-River-sand/mild-steel, plastic-silt/epoxy-coated-mild-steel, non-plastic-silt/epoxy-coated-mild-steel, and kaolinite/epoxy-coated-mild-steel interfaces at effective normal stresses between 3 and 7 kPa. Although the device provides accurate measurement at large shear displacement, the authors note that “The apparatus is not considered suitable for obtaining reliable estimates of the peak friction angle considering the high potential for strain non-uniformities along the shear length of the specimen especially at the initial level of shear displacement”. Amarasinghe, Wijewickreme, and Eid (2016) also conducted further tests on the same device in the

aim of collecting wider range of data and study the effect of plastic soils on the interface friction angle.

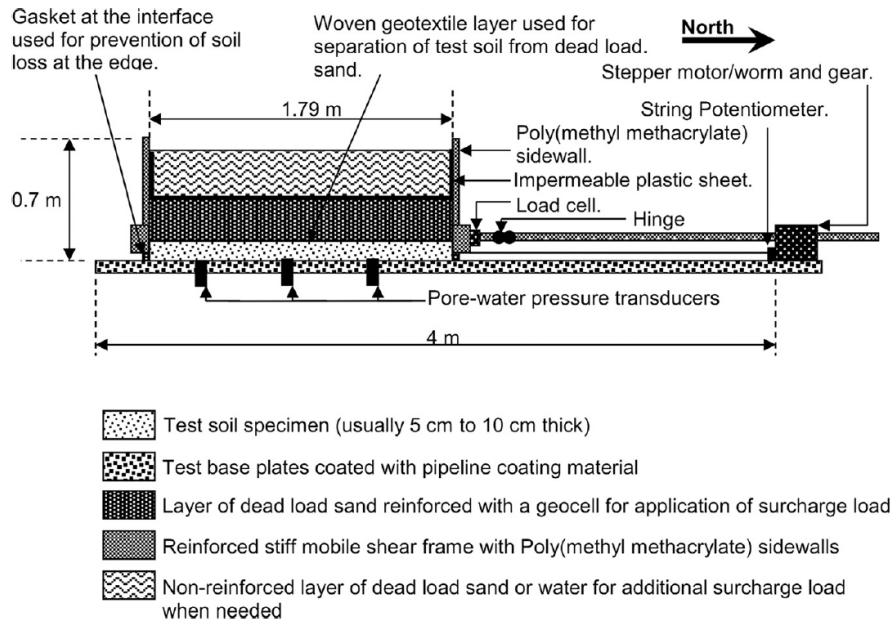


Figure 13 - Schematic diagram of the macro-scale interface direct shear test device and test setup.

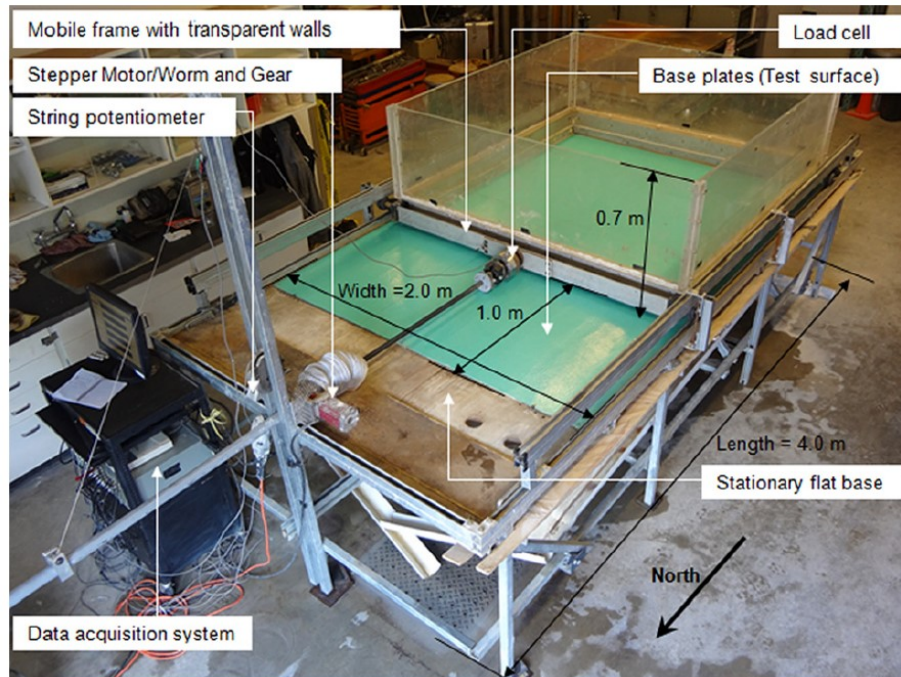


Figure 14 - Photograph of the macro-scale interface direct shear test device.

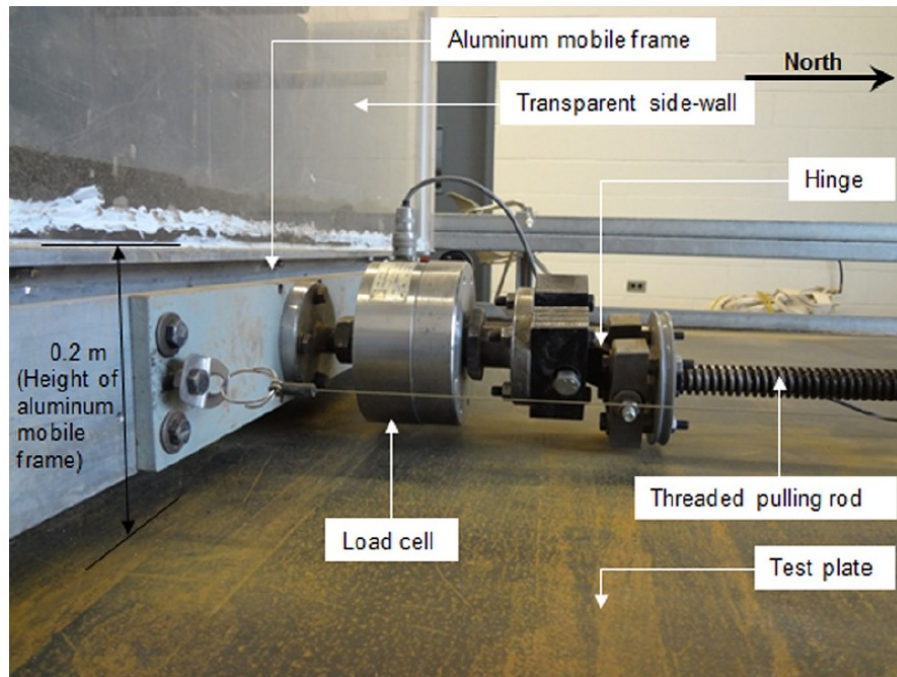


Figure 15 - Photograph illustrating the hinged connection between the load cell and the threaded rod transferring the tensile force to the mobile frame (note that the hinge shown is in a state with no load applied, hence the slack at the hinge in the diagram).

Boylan, White, and Brunning (2014) worked on a geotechnical centrifuge at the University of Western Australia (UWA) to model pipe-seabed sliding at low effective stress. With the characteristics of the centrifuge test, soil consolidation was performed at a much faster rate than what would be possible in physical models at unit gravity. The model pipe (140 mm in length and 20 mm in diameter) was placed in 650x390mm “strongbox” with 325 mm in depth. The pipe was attached to the loading arm through an S-shaped axial load cell to measure vertical forces and two bending strain gauges at the top of the loading arm to measure horizontal forces. Particles of fine-grained sand ($d_{50} = 160\mu\text{m}$) were glued to the pipe to achieve desired surface roughness. The friction coefficients measured in the study on a carbonate soil were between 0.7 and 3. To remove the effect of the soil resistance at both ends of the embedded pipe when sheared, the researchers have excavated the soil manually before starting of the shearing phase (figure 16).



Figure 16 - Test arrangement showing clearance of soil at pipe ends.

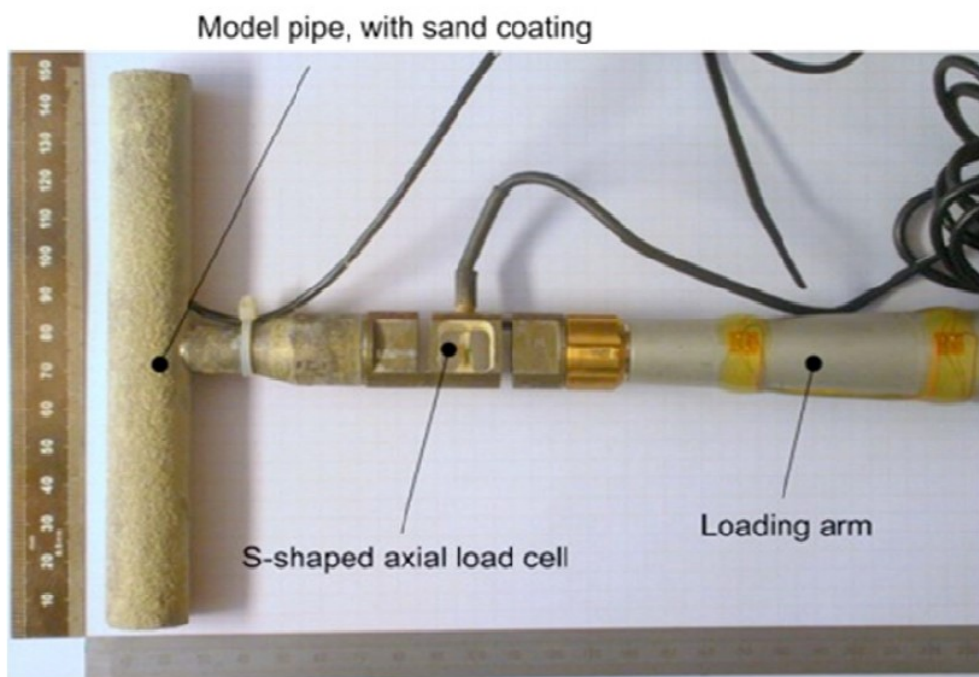


Figure 17 - Assembled model pipe, S-shaped axial load cell and loading arm

White et al. (2011) conducted a model test program in the University of Cambridge as a part of the SAFEBUCK JIP project. The model pipe was an 8m long plastic pipe that is 0.09m in diameter. The pipe was placed on a reconstituted soft natural clay in a 10x0.3m bed and 0.4m in depth and was dragged axially in both directions at displacement rates that range between 0.001 mm/s and 5 mm/s, with different pause periods between the series of sweeps. Two pore pressure transducers were installed at the bottom of the pipe to study the effect of drainage level on the axial interface resistance. The pipe (fully submerged) was free to move vertically and was dragged horizontally by an actuator through cables that ran over Teflon pulleys as seen in figure 18. A load cell was connected between the pipe and the cable to measure the horizontal force resistance, while vertical movement was recorded by two LVDTs placed on top of the pipe. The experimenters argued that that the ratio of the length of the pipe over its diameter $L/D = 89$ is enough to consider the soil resistance at both ends of the pipe as negligible.

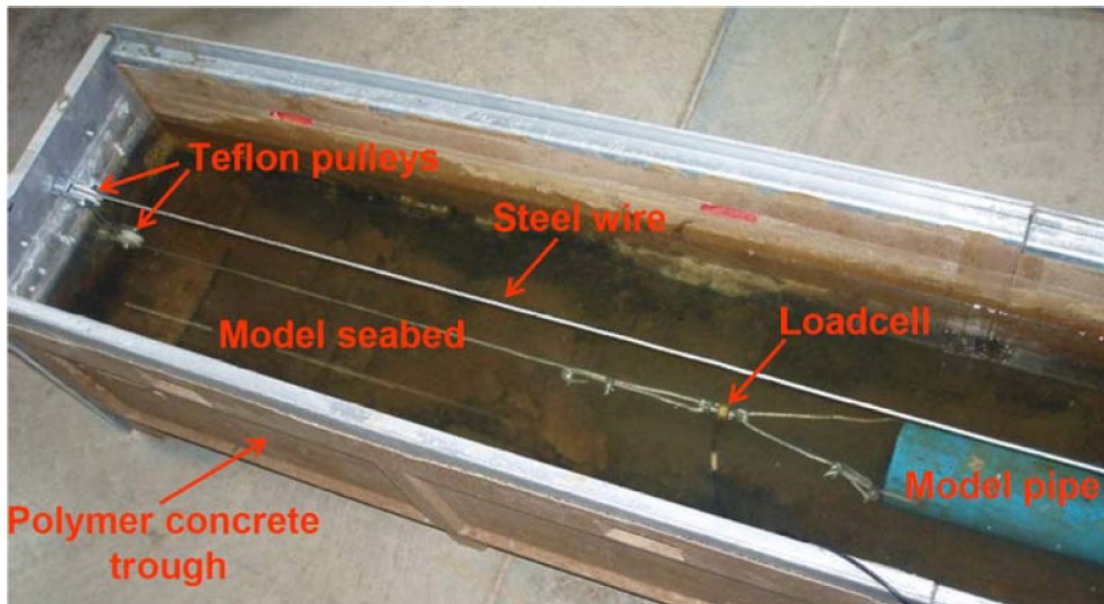


Figure 18 - Photograph of end of model pipe in test trough, showing pulling arrangement (University of Cambridge)

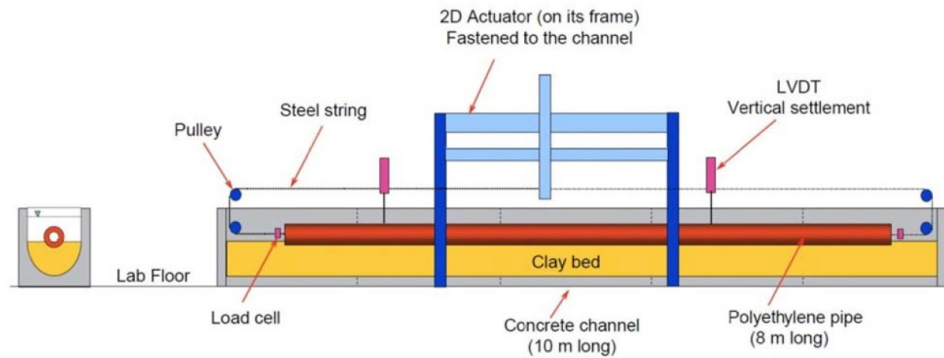


Figure 19 - Schematic diagram of the axial model testing (University of Cambridge)

2.3. In-situ testing

The best way to accurately measure the axial pipe-soil resistance is in-situ, replacing the need to sample offshore soils and re-constitute them in the laboratory which is time consuming especially at the early stages of design. Very few tools have been proposed in the literature for measuring the soil-pile interaction in-situ.

Stanier et al. (2015) proposed a device that aims at measuring the pipe/soil drained interface resistance. In principle, the concept involves dragging a tool on the seabed and measuring the friction mobilized between the tool and soil. The movement of the tool is controlled by an ROV (Remotely Operated underwater Vehicle) or by an electrical or hydraulic cylinder if the ROV is fixed in place. The sliding resistance is recorded by an attached load cell. Although the concept involves in-situ testing, all the reported tests in the study were conducted in the laboratory on dry sand and using three tools sandblasted to the same surface roughness: flat steel plate, steel pipe and steel chains. The tests were performed in a 2x2m pit with a thickness of 0.3m of dry silica sand, and under effective normal stresses between 4.8 and 6.6 kPa. An interpretation procedure is proposed to calculate the effect of the soil's passive force generated at the face of each embedded tool while dragging. The limitations of this device are (1) the

tool is dragged with in inclination angle which results in a non-uniform normal stress underneath it, and thus imprecise friction measurement results, and (2) the tool is dragged using a displacement rate of 50mm/s, and if the tool were to be actuated by an ROV thruster, it is difficult to reach slower constant displacement rates. While this fast rate of shearing might be adequate for testing sands, much slower displacement rates are needed for tests on clays, particularly if drained conditions are targeted. Third, the analyses of the results to determine the interface resistance is not straightforward due to the need for a mathematical interpretation technique to account for the end effects and shape effects.

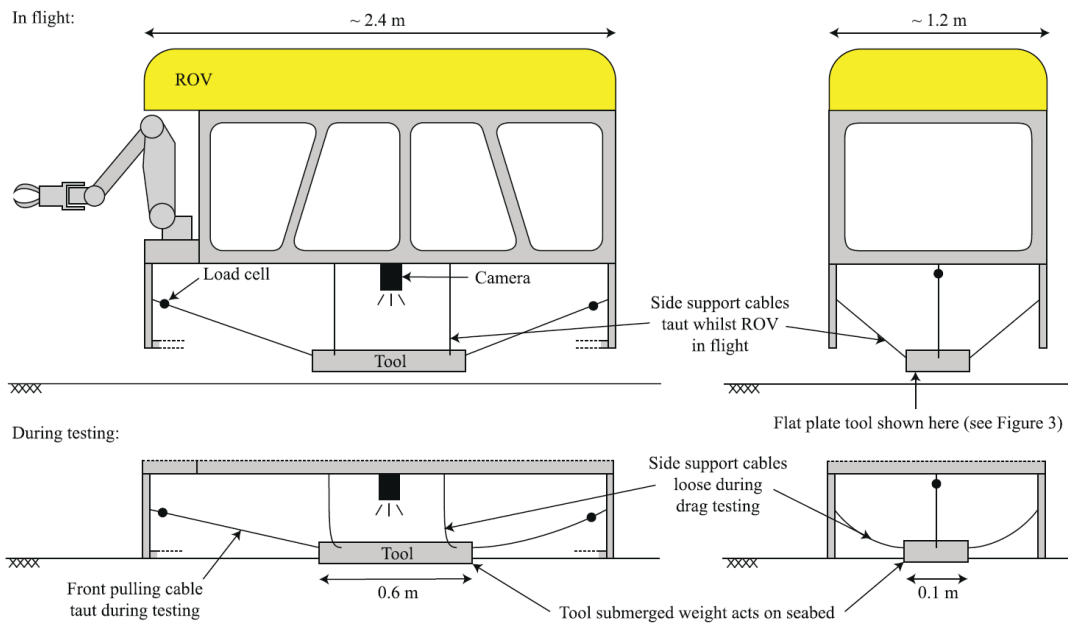


Figure 20 - Schematic of ROV-based drag test concept.

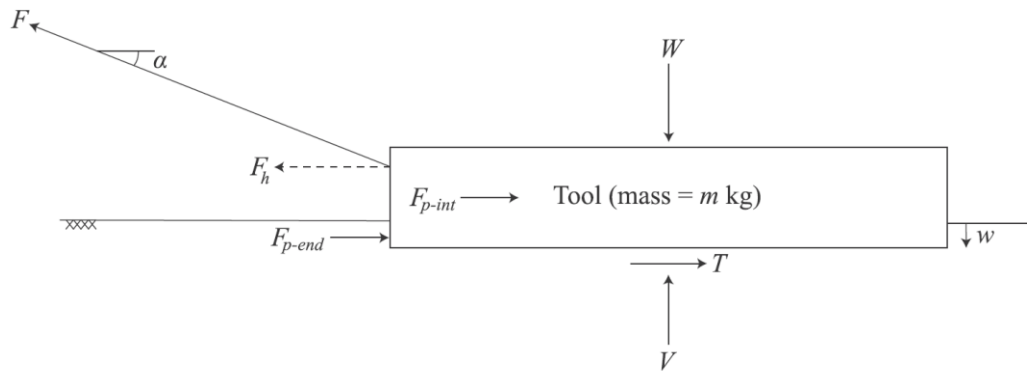


Figure 21 - Free body diagram of tool during testing.

Hill and Jacob (2008) presented an in-situ tool called the Fugro SMARTPIPE which was developed by Fugro (Geotechnical and Survey Services Company), BP (Major Oil & Gas Company), and the University of Cambridge in the aim of measuring the pipe-soil interaction parameters in situ. Unlike the previous equipment, the SMARTPIPE has been deployed at several offshore sites (White et al. 2010 and Ballard and Jewell 2013) and results and observations were presented following deployment. The equipment comprises of a mini T-bar penetrometer and a model pipe (1200 mm long and 225 mm in diameter) mounted on a steel frame. The frame is deployed from a vessel and is equipped with a settlement plate, a camera, roll and pitch sensor etc. The pipe consists of two end dummy sections that eliminate end effects and a central measurement section (776 mm long) that is connected to the two end parts by means of triaxial load cells to measure the vertical, lateral and axial forces acting on the central section. The pipe is actuated by a hydraulic system and is able to move axially at a rate that ranges between 0.005 mm/s and 1.15 mm/s, and laterally between 0.1 mm/s and 0.8 mm/s. Nine pore water pressure sensors are also attached to the bottom of the central pipe section to measure the change in excess pore water pressure during consolidation and shearing stages, and determine the effective normal stresses throughout the test. The

pipe interface is polypropylene coated and has an average surface roughness of 5-10 μ m. The limitations of this equipment are that the data collected by the instrumentation has to be transferred to the vessel through a fiber optic cable, which makes it vessel-dependent and results in higher cost especially if the tested soil requires more time for initial consolidation stage and for waiting time between cycles of shearing. Moreover, although the model pipe can be actuated by displacement-rate control or load-controlled, the results and observations from the tests showed that the limitation in the hydraulic system made it difficult to maintain constant vertical loading throughout the tests.

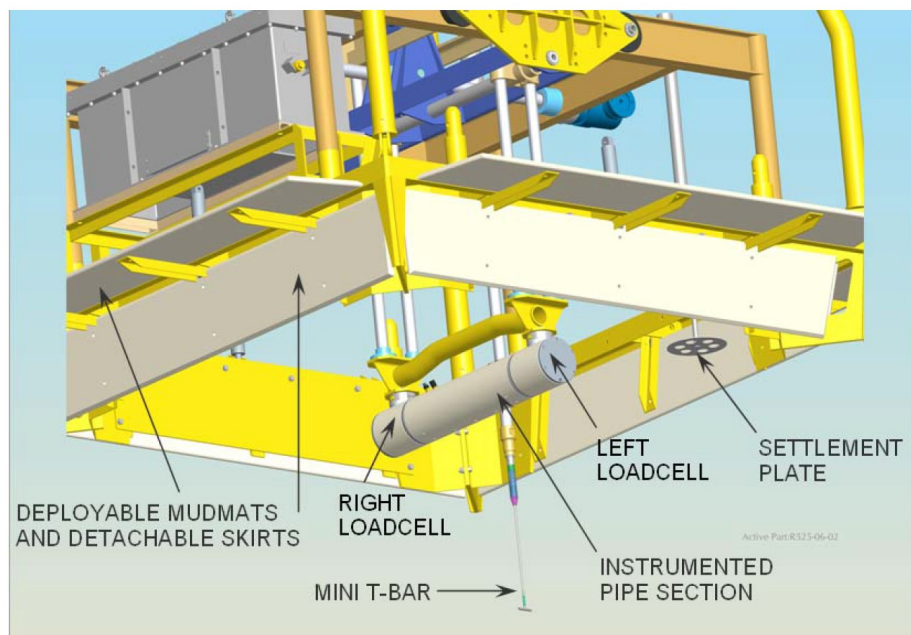


Figure 22 - Schematic view of Smartpipe tool

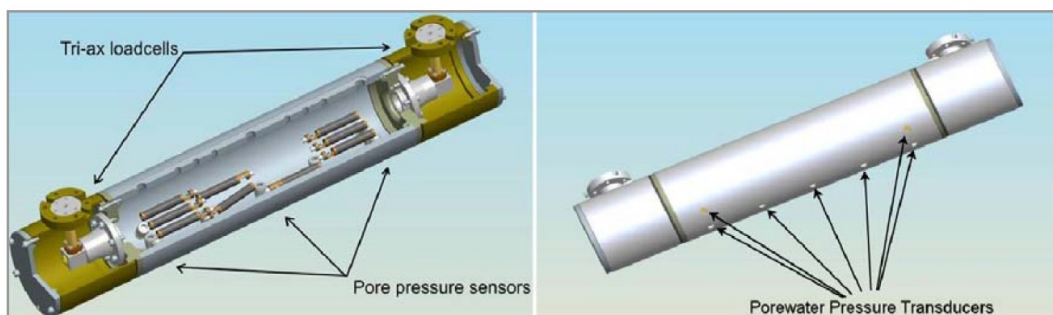


Figure 23 - Cutaway view of model pipe and pore pressure transducers on pipe surface

2.4. Pipe-Soil Interaction Framework

White et al. (2012) and Hill et al. (2012) have used a set of data from in situ tests (Box Core, T-bar, SMARTPIPE), onshore model tests (small and large model) and laboratory tests (tilt table and interface shear box) to calibrate a theoretical framework for axial pipe-soil resistance, which was later slightly modified by Boukpeti and White (2017).

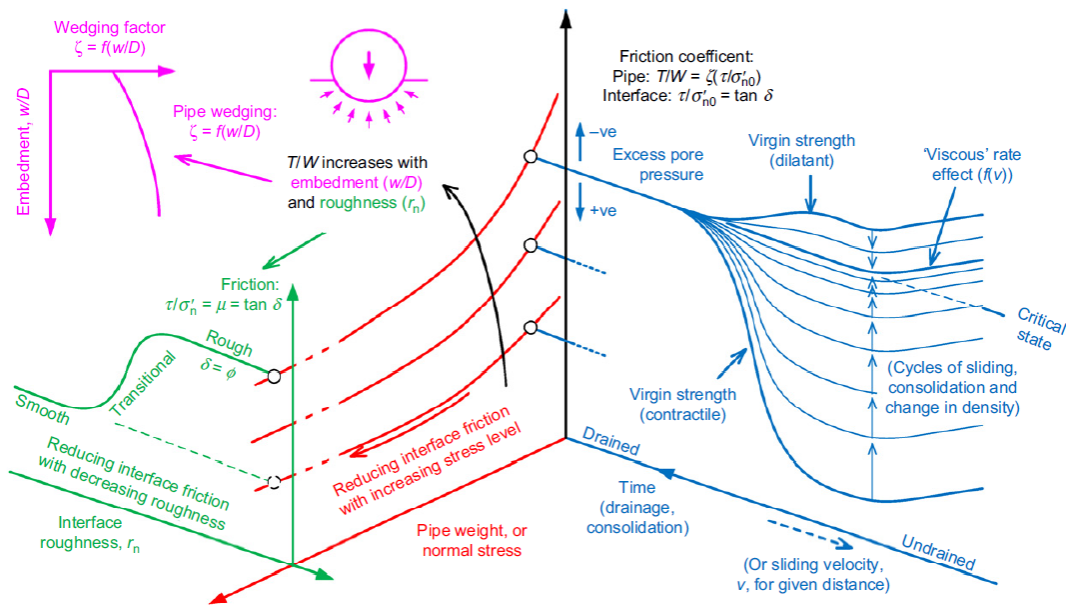


Figure 24 - Axial pipe-soil interaction framework

The framework is comprised of four elements as indicated in Figure 24. These elements include an undrained-drained transition relationship (blue), an effective stress failure envelope (red), an interface ‘efficiency’ related to roughness (green) and a ‘wedging’ effect for curved pipe surfaces (purple). The wedging effect is introduced in White and Randolph (2007) and it accounts for the additional normal force beyond the weight of the pipe that need to be considered due to the pipeline shape, with the wedging factor ζ ranging between 1 and 1.27 depending on the pipe’s embedment depth. The framework highlights how the smooth and rough interfaces give low and high friction coefficients, respectively. Similarly, the failure envelope tends to be

curved for low values of effective stress, showing an increase in friction coefficient with decrease in normal stresses. Lastly, the framework uses the concept of critical state soil mechanics to assess how loading history, excess pore pressure and consolidation during cycles of shearing affect the transition from undrained to drained behavior, and thus affecting the interface shear resistance through these cycles. The theoretical framework has permitted to narrow the estimate range of friction coefficients; however, it still needs further validation by performing tests on more soil types.

Randolph et al. (2012) provided a theoretical framework for assessing the axial pipe-soil interaction, focusing on catching the variation in friction resistance with the rate of axial movement and its duration leading to soil contraction underneath the pipe in case of normally consolidated clay. Few years later, Low et al. (2017) presented a calculation procedure that permits for the calculation of the peak and residual interface shear strength throughout the lifetime of the pipeline operation (Figure 25).

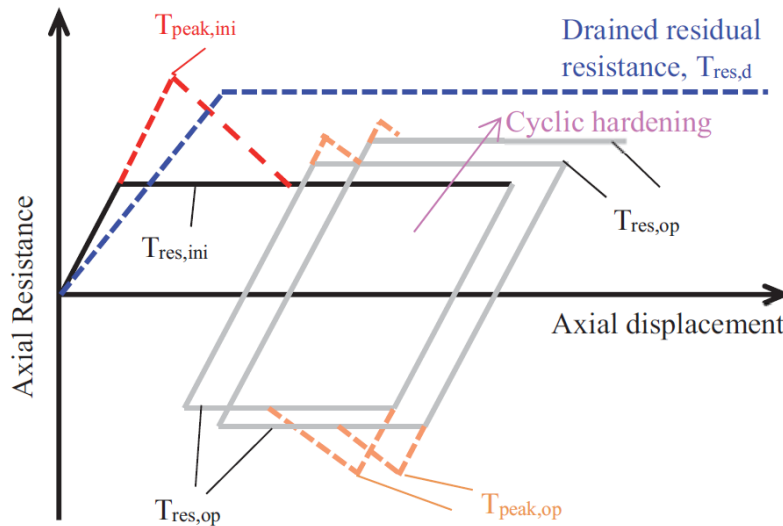


Figure 25 - Schematic for axial resistance displacement response

CHAPTER 3

TESTING MATERIALS

3.1. Soils

In this study, three soils have been used in testing with similar characteristics of the ones found in the offshore environment: A Natural Clay (NC) with low plasticity, a High Plasticity Clay (HPC) and a synthetic Kaolinite (KAO), having a 2.63, 2.78 and 2.56 specific gravity, respectively. Both the HPC and KAO are constituted of 100% fines with all their particles passing sieve no. 200 (0.075mm). On the other hand, the NC is a mix of 26% sand and 74% fines. The NC has a relatively low plasticity index $PI=12.5\%$ compared to the HPC with $PI=54\%$, whereas the KAO has a PI of 26%. NC, HPC and KAO are classified as CL, CH, and MH respectively as per the Unified Soil Classification System, USCS (ASTM D2487). The characteristics of these three soils are summarized in Table 1.

Table 1. Soils Characteristics

Soil	G_s	Size fraction (%)			USCS	Atterberg Limits (%)		
		Sand	Silt	Clay		LL	PL	PI
Natural Clay	2.63	26	36	38	CL	28.9	16.4	12.5
High Plasticity Clay	2.78	0	50	50	CH	83	29	54
Kaolinite	2.56	0	8	92	MH	65	39	26

Slurry specimens are prepared by thoroughly mixing the oven-dried samples at water contents equal to or greater than their liquid limits. The NC is mixed at a water content of 29%, whereas the HPC and KAO are mixed at 100% water content. After the mixing, to ensure homogeneity, each reconstituted sample is left in a sealed plastic bag

for a duration of time prior to testing, as per ASTM D3080 section 7.2 (Table 2). A minimum of 18 hours standing time for the NC, and a minimum of 36 hours for the HPC and KAO was used. On the day of testing, the sealed plastic bag is opened, and the soil is remixed thoroughly before being placed in the shear box for testing. To ensure consistency and repeatability the same quantity of soil was placed into the shear box at each of the four normal stresses used in testing.

Table 2: Stand time for reconstituted sample as per ASTM D3080 section 7.2.

USCS Classification (D2487)	Minimum Standing Time, h
SW, SP	No Requirement
SW-SM, SP_SM, SM (>5% fines)	3
SC, ML, CL, SP-SC	18
MH, CH	36

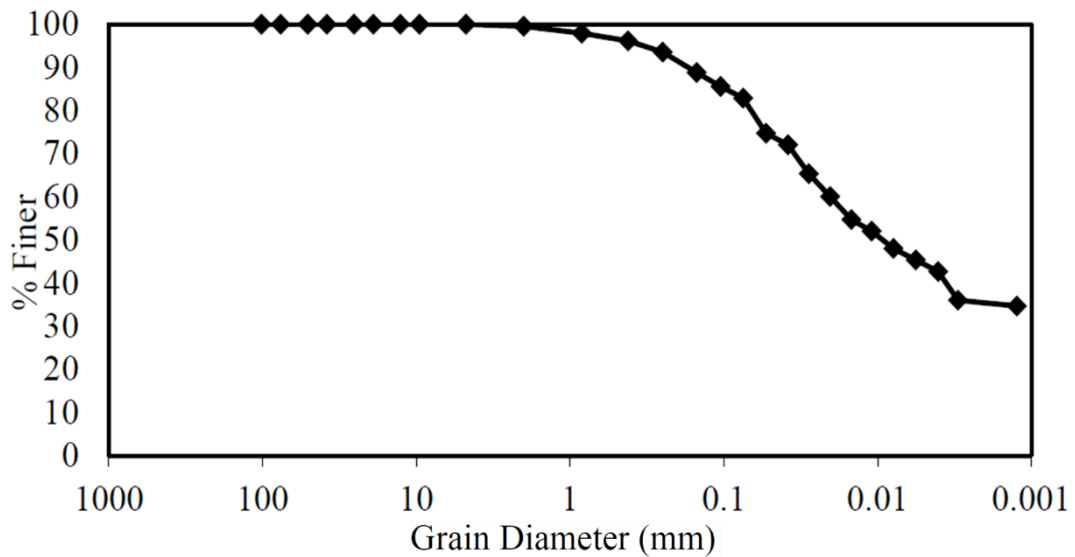


Figure 26. Particle-size distribution of the Natural Clay

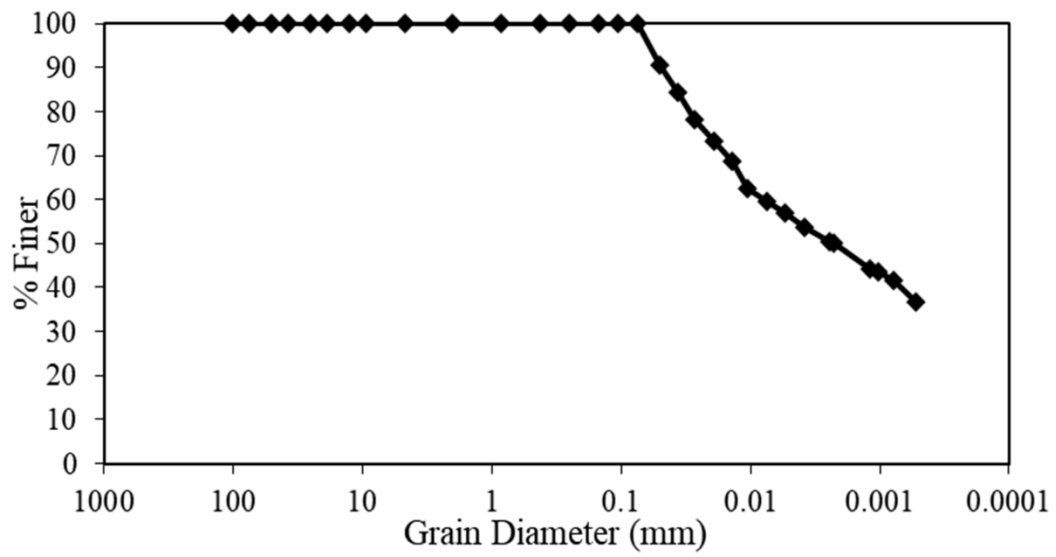


Figure 27. Particle-size distribution of the High Plasticity Clay

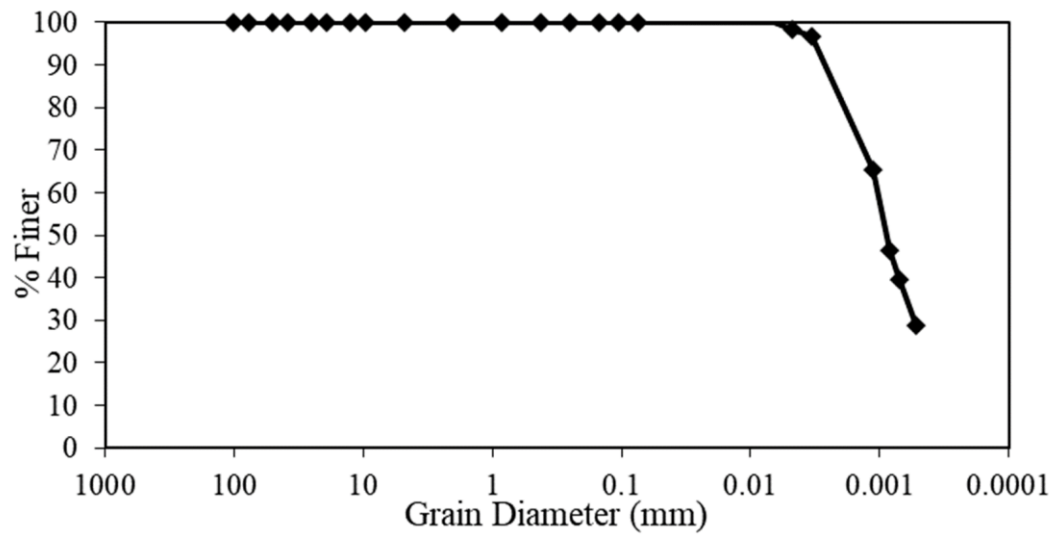


Figure 28. Particle-size distribution of the Kaolinite

3.2. Interfaces.

Three types of interfaces were tested: Plexiglass, Stainless Steel and Sandpaper having a surface roughness R_a of $0.003 \mu\text{m}$, $0.08 \mu\text{m}$ and $3.5 \mu\text{m}$, respectively, measured using a profilometer. Sheets of $300 \times 300 \text{ mm}$ for each interface were prepared for the tilt table tests and smaller ones of $90 \times 60 \text{ mm}$ size were fitted into the lower half of the shear box for the interface direct shear tests (Figure 29). The Sandpaper was

glued to a plastic sheet with epoxy resin to guarantee that no air bubbles are entrapped between the Sandpaper and the lower plate, and was also folded and glued to the opposite side of the plate to prevent any sliding of the Sandpaper on the plate during testing (Figure 30). In this study, the Plexiglass and Stainless Steel will be referred to and considered as smooth interfaces, whereas the Sandpaper will be designated as the rough interface.

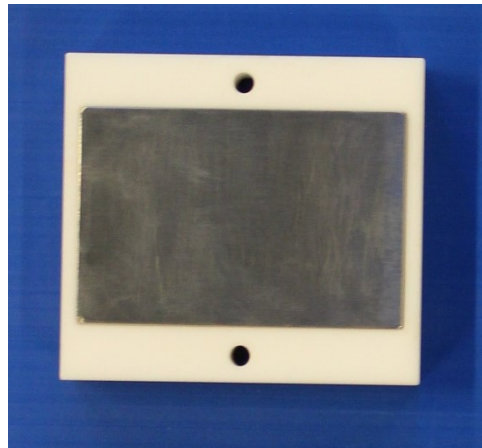


Figure 29. 90x60 mm size Stainless Steel interface fitted into the lower shear box of the interface direct shear.

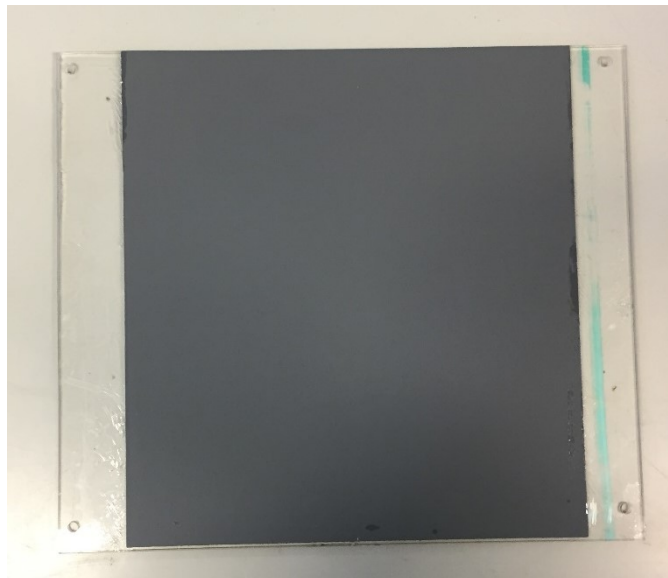


Figure 30. Sandpaper glued to a plastic sheet for Tilt Table testing.

CHAPTER 4

INTERFACE DIRECT SHEAR TESTING

4.1. Modified Direct Shear Apparatus.

To conduct the interface direct shear testing, a conventional direct shear apparatus was modified to limit the system's mechanical friction and suit the low confining pressure applications. The friction is mainly due to the box-interface sliding resistance, the weight of the shear box and the sample loading technique (level arm and eccentricity). Accordingly, the steel shear box was replaced by a custom-fabricated Teflon box that has a lighter weight and a lower sliding resistance. Moreover, dead weights were put directly on top of the sample via a frictionless loading frame ensuring that the weights are perfectly centered, and the applied normal stress on the soil sample is uniform. The lower half of the shear box was designed to accept the interface, whereas the upper half has four screws with Teflon caps to adjust the gap between the two halves and minimize friction during sliding against the lower half. In addition, the measurement instruments were upgraded to guarantee accurate readings of the very low shear forces (Omega load cell of 50 N capacity and 0.05 N accuracy) and the settlements and horizontal displacements (LVDT with 0.001 mm accuracy). In addition to the above, another lower half Teflon box similar to the original steel box was also fabricated to perform direct shear tests at low confining pressures. Figure 31 and Figure 32 show the modified direct shear machine with the new Teflon shear box.

As shown on Figure 33 and Figure 34, a graphical code was created on the LabVIEW software, while using an NI (National Instruments) Digital I/O data

acquisition system to collect and save the data from the load cell and LVDTs during consolidation and shearing phases.

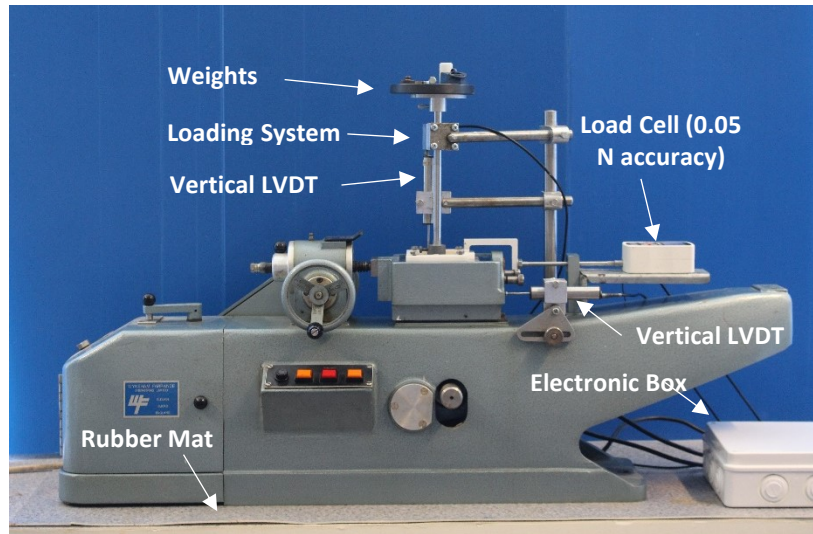


Figure 31. Modified Direct Shear Machine (Modified components)

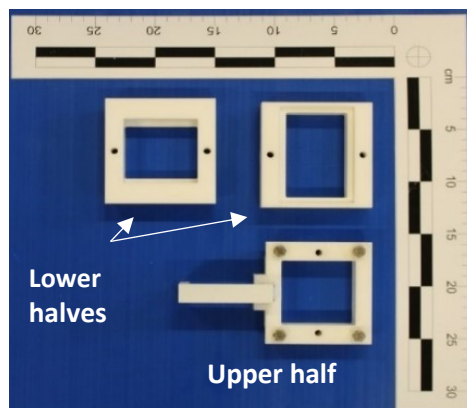


Figure 32. Custom-fabricated Teflon shear box

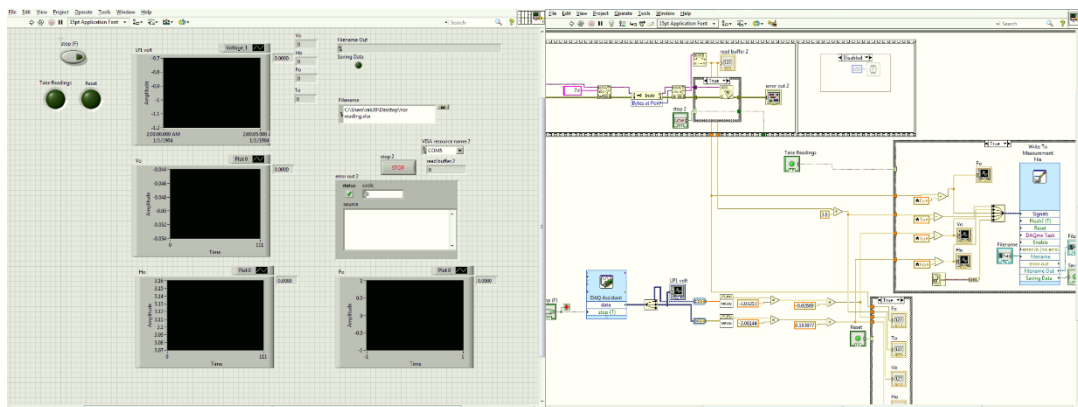


Figure 33. LabVIEW code

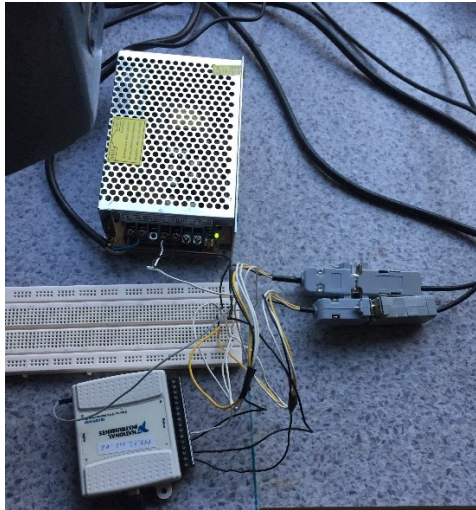


Figure 34. Data acquisition system placed inside the electronic box

4.2. Testing procedure (sample preparation, consolidation, and shearing phase).

The soil sample is prepared by mixing the soil thoroughly at the desired water content to ensure homogeneity. After 24 hours, the mixed soil was placed inside a 1 cm thick square cutout having an area of 60x60 mm, before transferring it to the upper half of the Teflon shear box. A filter paper and a porous stone were placed on top of the specimen, along with the loading system and the LVDT measuring vertical displacements. Dead weights were then added on top of the loading arm to reach the desired confining pressure (1.7, 2.5, 4.5 and 6.1 kPa) and the monitoring of the consolidation phase starts. Once the primary consolidation is completed, the screws are loosened and a gap of around 0.7 mm is created for the interface tests, where a gap having the maximum soil particle size is adopted for the soil strength test.



Figure 35. Sample preparation.

From the consolidation graphs, the time to failure that ensure drained loading conditions is computed using Equation 1 (as per ASTM D3080 section 9.10.1):

$$t_f = 50 t_{50} \quad (1)$$

Where:

t_f = total estimated elapsed time to failure in seconds.

t_{50} = time required for the sample to achieve 50% consolidation.

The shearing rate is chosen to be slower than the one calculated from Equation 2 so that no excess pore pressures are generated during the shearing process.

$$R_d = \frac{d_f}{t_f} \quad (2)$$

Where, R_d = shear rate, mm/s.

d_f = estimated lateral displacement at the peak failure, mm.

Based on the consolidation data, the shearing rates were selected to be 0.00004 mm/s for interface tests and 0.00005 mm/s for the clay tests. The shearing phase was terminated when the reductions in the shear stresses with displacement stabilized indicating the mobilization of the residual interface strength, generally after reaching 3-5mm. It should be noted that when the Natural Clay was tested, several tests were conducted up to displacements of 10 mm. The results from these tests confirmed that

terminating the tests at displacements of 3mm is adequate for the purpose of estimating the residual strength for the remolded clay specimens that were consolidated from a slurry.

Note: In the direct shear and interface direct shear tests, the shearing rates were determined as per section 9.10.4 of ASTM D3080. However, after repeating some tests at the same confining pressure but with slightly higher shearing rates, the recorded shearing strength and behavior have remained the same and negligibly changed. To save time on the very lengthy testing, while ensuring that the used higher shearing rate gives the same results as the one originally determined as per ASTM, the following two shearing rates were adopted in all direct shear testing: 0.00004 mm/s and 0.00005 mm/s, which are still considered very slow when compared to the shearing rates adopted in the literature for interface testing using the same type of materials (soil and interfaces).

4.3. Important considerations to minimize friction for direct shear testing at low normal stresses:

- The modified direct shear apparatus has been detached from the original table supporting it and was placed on solid ground. A rubber mat has been placed underneath it to avoid unwanted vibration on the sensitive load cell and LVDTs resulting in inaccurate measurements (Figure 31).
- The track, on which the shear box bowl is moving during the shearing phase, should be checked regularly for rust accumulation, and treated with the like of WD-40 spray material to avoid mechanical friction resulting from it.

- All components of the data acquisition system, the data processing device (computer), the load cell, the LVDTs, and the direct shear motorized section shall be connected to a safety powerline at all time during the test.
- Although the interface is cut and trimmed to fit tightly into the lower half of the shear box, strong tape is used to attach it at both side in the direction of the shearing to prevent any minimal movement and reduction in the recorded resistance (Figure 36).

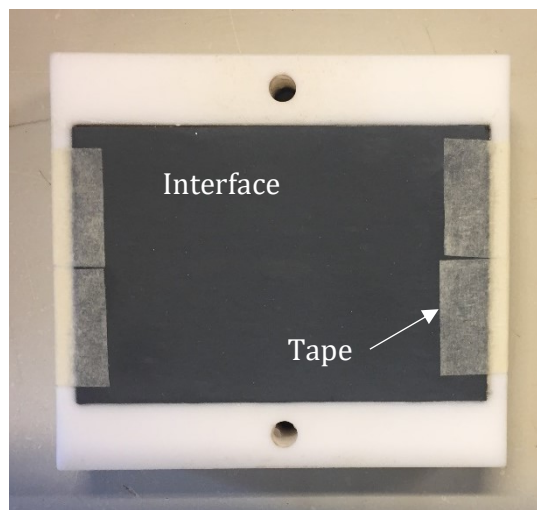


Figure 36. Tape attaching the interface tightly to the lower shear box.

- The filter paper that is placed between the soil sample and the porous stone should be trimmed accurately to the size of the shear box. This step of the test could be time-consuming and very well underestimated, as having a larger filter paper than the shear box area will increase friction with the inside walls of the shear box, whereas having smaller filter paper will result in the soil specimen coming out from side of the filter paper when the specimen is loaded. Note that cutting and trimming of the filter paper should be conducted after damping it with water, as the paper tends to stretch and slightly increase in size when damped (Figure 37).

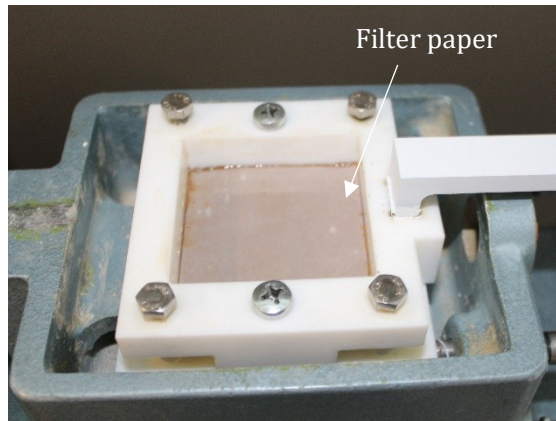


Figure 37. Filter paper trimmed to the size of the shear box.

- The porous stone should be cut 1mm from each side to prevent contact with the shear box's inside walls and avoid vertical friction during the consolidation and shearing phases (Figure 38). Same is applicable to the loading plate shown in Figure 40.

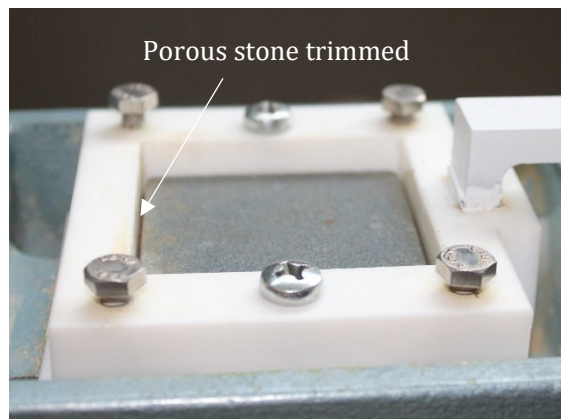


Figure 38. Porous stone trimmed.

- To minimize vertical friction between the soil specimen and the inside walls of the shear box, oil shall be spread lightly on the inside walls while keeping an oil free distance of 2mm from the interface surface, as any protruding of oil to the interface during testing will weaken the shearing plane and affect the resistance's readings (Figure 39).

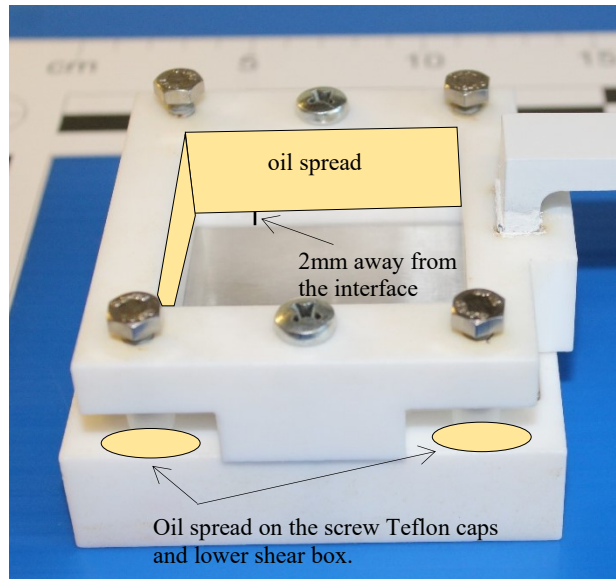


Figure 39. Spreading of oil on to minimize friction.

- To minimize the horizontal friction, oil shall be applied to the Teflon screw caps of the upper shear box sliding against the lower shear box part, while also applying oil on the track/sliding area of the lower shear box (Figure 39).
- Placing the dead weights on top of the loading system should be done in a slow and delicate manner.
- After completion of the consolidation phase, the upper shear box is raised from the lower part and then attached to the load cell. The screw nut attaching the upper shear box and the load cell should be tightened in a way to connect them both, but not excessively as it can create a built-up tension and immediately shear the specimen once the screws holding the upper and lower shear box together are removed (Figure 40).

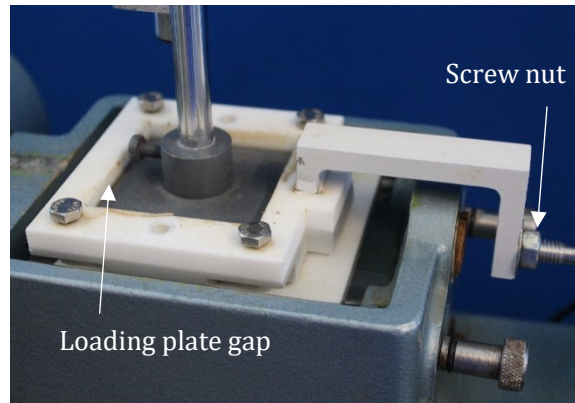


Figure 40. Smaller area of loading gap, and screw nut used to connect the upper shear box and the load cell.

- To reduce vibration and avoid shearing of the specimen while detaching the shear box parts from each other, oil shall be applied to the screws' threads joining both parts together to avoid application of excessive force during the pull out process of the screws after the consolidation stage is completed.
- Depending on the type of soil tested, the consolidation and shearing phases may take days, and the water inside the shear box bowl will eventually evaporate. Adding water should be performed in a slow and delicate manner to not disturb the very sensible and accurate load cell readings.

4.4. Measurement of the horizontal and vertical friction.

Although having a custom-fabricated Teflon shear box minimizes the friction significantly, the remaining vertical and horizontal frictions shall be measured and accounted for in the data analysis and determination of the interface shearing resistance. For measurement of the vertical friction, a special setup was created with a steel plate connected to a load cell from the bottom side and receiving the soil specimen and applied normal stress from the top using the same loading system of the modified direct shear setup (Figure 41 and Figure 42).



Figure 41. Vertical measurement setup.



Figure 42. Vertical measurement setup closer view.

Below Table 3 presents the results of the measurements, showing the difference between the theoretical vertical load applied on the specimen and the actual measured load felt by it at the level of the shearing plane.

Table 3. Difference between theoretical and actual measured normal stress.

Normal stress (kPa)	NC	HPC	KAO
1.7	11%	6%	6%
2.45	11%	6%	6%
4.26	9%	6%	6%
6.1	7%	6%	6%

For the measurement of the horizontal friction, shearing resistance of the upper and lower Teflon shear box sliding against each other was recorded, obviously without a soil specimen inside the box, but having the shear box bowl full of water as in the case of all direct shear tests in this study. The measured horizontal friction was 0.3 N at 0.00004 mm/s shearing rate.

Figure 43 compares the drained residual friction angle with normal stress when the vertical and horizontal friction were considered in the analysis (in black) and when they were ignored (in red).

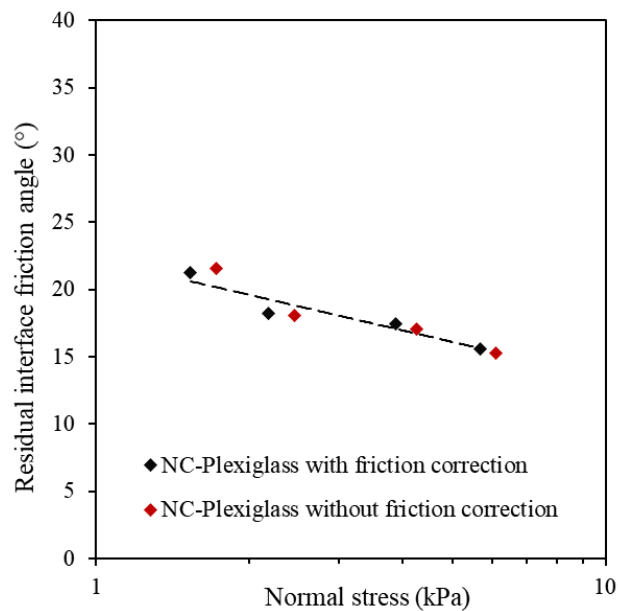


Figure 43. Comparison between interface friction angle with and without correction for vertical and horizontal friction

CHAPTER 5

TILT TABLE TESTING

5.1. Tilt Table Apparatus.

A Plexiglass Tilt Table was fabricated to measure the residual pipeline-soil interface strength under drained conditions. The apparatus is composed of a Plexiglass plate of 450x450 mm area, hinged to the base at one side, while the other side is attached to a manual gear through a cable. The plate can be lifted by rotating the gear and a maximum inclination angle of 45° can be read on the curved vertical plate as shown in Figure 44. The tested interfaces with a size of 300x300 mm are typically fixed on the plate using four screws except for the sandpaper that is glued to a thin plastic sheet using epoxy and then fixed to the tilt table. After placing the soil and applying the target normal stress, the tilt table is submerged inside a Plexiglass water bath to ensure full sample saturation.

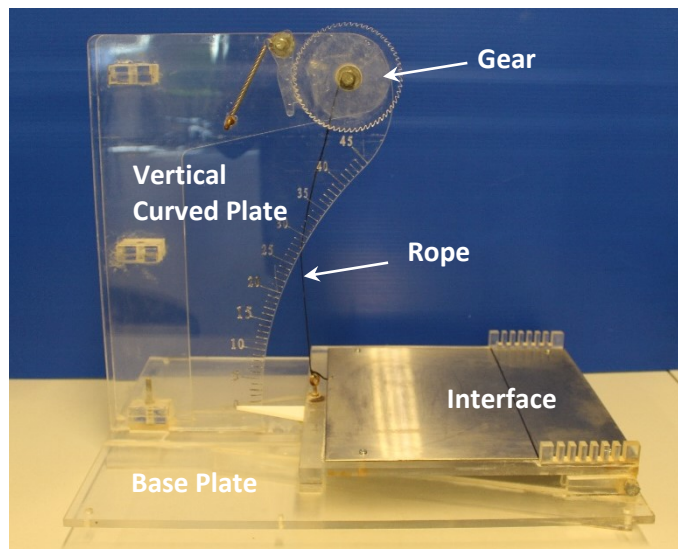


Figure 44. Tilt table testing setup.

5.2. Testing Procedure.

As for the direct shear testing, the oven-dried soil is mixed at the desired water content and left in a sealed plastic bag for a minimum period of time before testing, as per ASTM D3080 section 7.2. Then, a 2 mm thick layer of soil was spread over the interface with an area of 150x150 mm that matches the size of the steel loading plate used to apply the desired normal stress (Figure 45). The consolidation phase was initiated by placing the loading plate on top of the soil as show in below Figure 46.

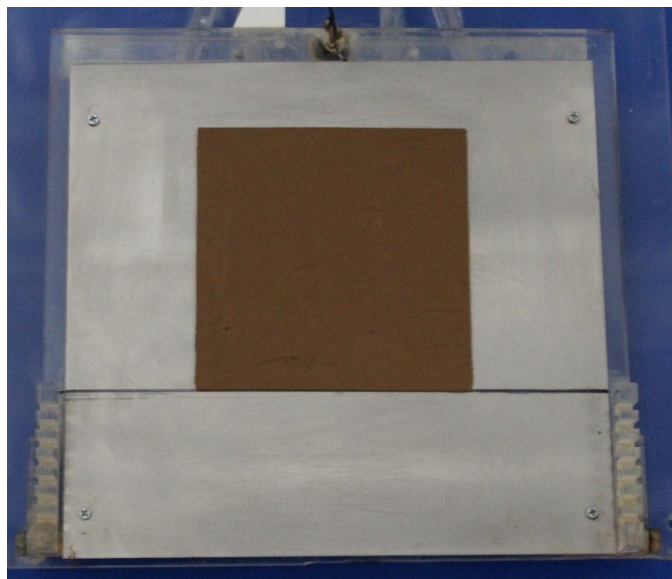


Figure 45. Spreading of the 2mm specimen on the interface.

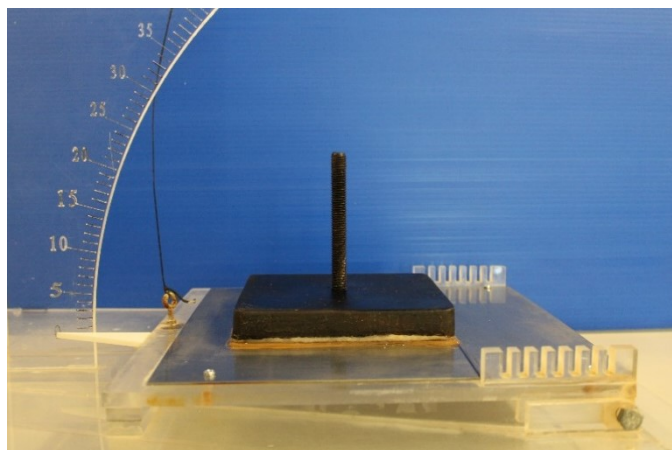


Figure 46. First phase of consolidation under loading plate only.

Once 95% of the consolidation was achieved under the weight of the loading plate, the whole setup was placed inside the water bath and dead weights were added on top of the loading plate with a specific offset from the center to reach a uniform normal stress at failure while minimizing eccentricity (Figure 47). This offset in the center of gravity of the loading was created by attaching spacers of different thickness to the loading plate. One trial test was done for each normal stress to select the correct offset distance that ensures uniform normal stresses on the sample at failure. The sample was then left enough time to achieve a degree of consolidation of 95% under this normal stress. This time was calculated from Equation 3.

$$t_{95} = \frac{T_{95}H^2}{C_v} \quad (3)$$

Where $T_{95} = 1.129$; C_v = coefficient of consolidation obtained from the consolidation phase of the interface direct shear tests at the desired normal stress (mm^2/s), and H = the sample thickness (2 mm).

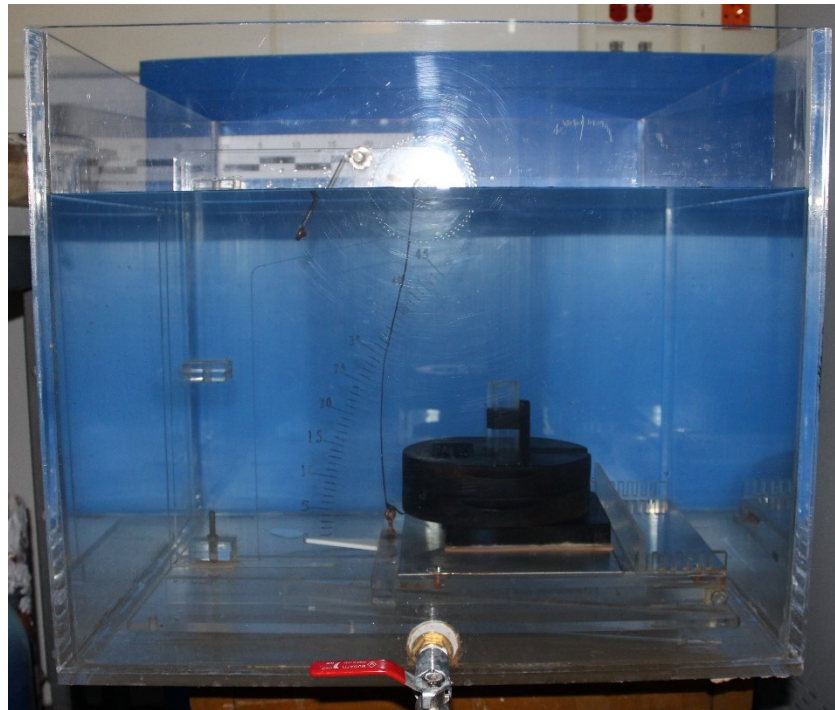


Figure 47. Tilt table setup placed inside the Plexi water bath.

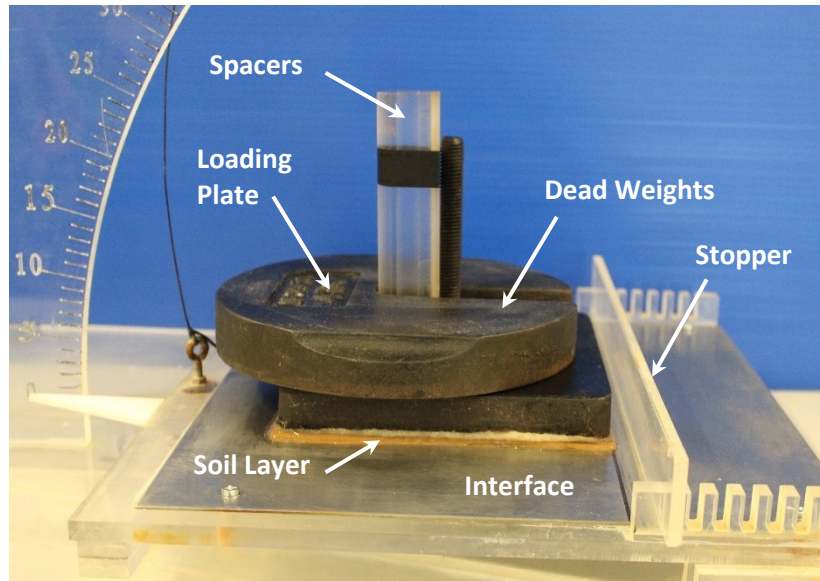


Figure 48. Tilt table setup as is inside the water bath.

After the consolidation, shearing begins by lifting the Plexiglass plate slowly enough in order to allow any generated excess pore water pressures at the interface to dissipate. The rate of shearing is selected in a way to maintain constant level of deformation and drained conditions. The inclination increments are basically 5° , 3° , 2° followed by 1° increments until slippage occurs. From the trial test, a preliminary estimate of the failure angle can be obtained. Thus, an approximate number of inclination increments can be set. Based on this number, the minimum waiting time at each increment can be deduced by dividing the time to failure (from equation 1) by the number of increments. Once the sample slips, a stopper rod will block its displacement at 10 mm. Afterwards, the plate is lowered 10° and left for 10 min and the whole procedure is repeated 7 times until 70 mm of displacement are attained. The last slippage angle is considered as the residual interface angle (α) and the corresponding effective normal stress and the shear stress at failure can be calculated using Equations 4 and 5 respectively.

$$\sigma' = \frac{W'}{S} \cos(\alpha) \quad (4)$$

$$\tau' = \frac{W'}{S} \sin (\alpha) \quad (5)$$

where W' = Submerged weight on the sample (sum of the loading plate and the dead weights), kg and S = area of the sample, mm^2 . Figure 49 clarifies the slipping phase when performing a tilt table test.

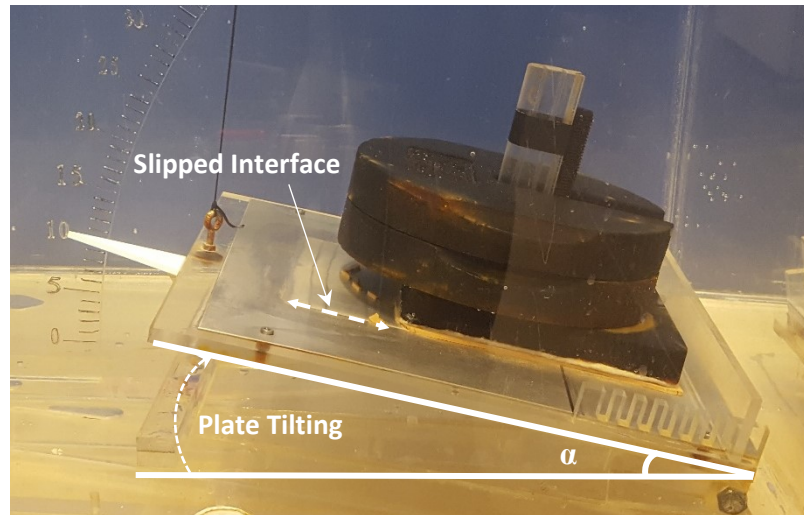


Figure 49. Slipping phase on the tilt table.

5.3. Important considerations for tilt table testing:

- It is recommended to have a custom-fabricated template with a specific thickness (here 2mm thick) and cut out area (150x150mm in this study) to help in spreading of the soil on the interface in a consistent way for all tests.
- The total dead weight and spacers for eccentricity should not be added before placing of the tilt table apparatus inside the water bath, as this increases the normal stress at the consolidation stage because of having the total weight applied on the soil specimen and not the same submerged weight applied inside the water bath.

- When transferring the tilt table test setup into the water bath, and as the setup can be heavy depending on the applied weights, care should be exercised to not disturb the soil specimen during transfer and insertion into the water.
- During the shearing stage, increments duration should not be rushed to ensure full dissipation of water and avoid undrained shearing of the soil specimen.

CHAPTER 6

TESTING CONCEPT

One of the objectives of this study is to investigate whether the residual interface strength at low confining pressures can be reached using typical interface direct shear testing. Since the tilt table device allows for high displacements under fully drained conditions without any mechanical friction, its results are widely adopted in order to obtain the residual interface resistance. However, the typical direct shear setup is limited by the sample size, the device's mechanical friction, and the maximum displacement which can be reached. However, it can be argued that following the elimination of most of the inherent setup friction and performing tests at a very slow shearing rate as described before, a comparison between the two techniques is possible and can provide valuable insight. Thus, tilt table and direct shear tests were performed at four different low confining pressures: 1.72, 2.44, 4.26 and 6.1 kPa for three interface types using the Natural clay. In this manner, the dependency of the interface resistance on the normal pressure and the influence of the interface roughness can also be investigated. Further tests, using the High Plasticity Clay and Kaolinite, were also performed to confirm the findings.

CHAPTER 7

EXPERIMENTAL RESULTS AND DISCUSSION

7.1. Consolidation response.

The coefficient of consolidation, c_v , of the NC, HPC and KAO was estimated from the consolidation phase of the interface direct shear tests by considering one-way drainage conditions using Equation 6:

$$c_v = 0.196 \frac{H^2}{t_{50}} \quad (6)$$

With a sample thickness of 10 mm and t_{50} of approximately 500 seconds, the average c_v was calculated to be approximately 1.1 m²/year for the NC. For the HPC and KAO, it was estimated to be around 0.25 m²/year and 1.3 m²/year, respectively.

Figures 51 to 60 show the consolidation graphs of the NC-Plexi, NC-Steel, NC-Sandpaper, HPC-Steel, HPC-Sandpaper, KAO-Steel, KAO-Sandpaper, NC-NC, HPC-HPC and KAO-KAO, under four low normal stresses: 1.7, 2.45, 4.26 and 6.1 kPa.

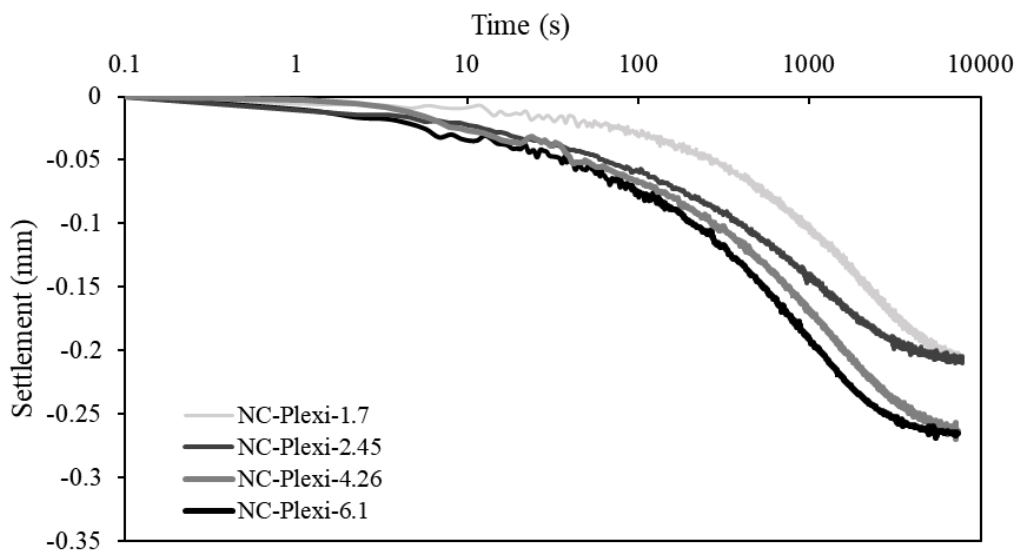


Figure 50. Consolidation of Natural Clay - Plexiglass (10mm thick specimen)

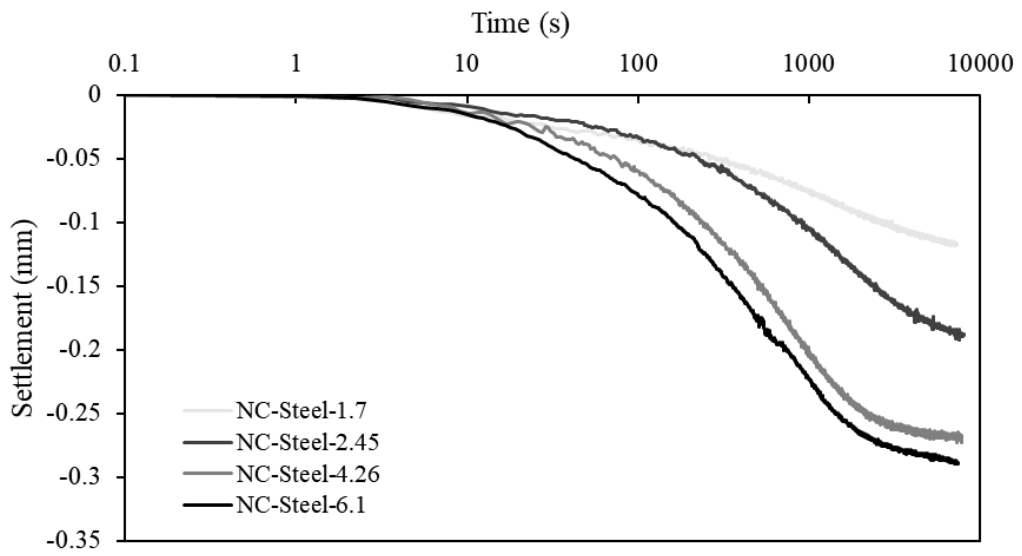


Figure 51. Consolidation of Natural Clay - Stainless Steel (10mm thick specimen)

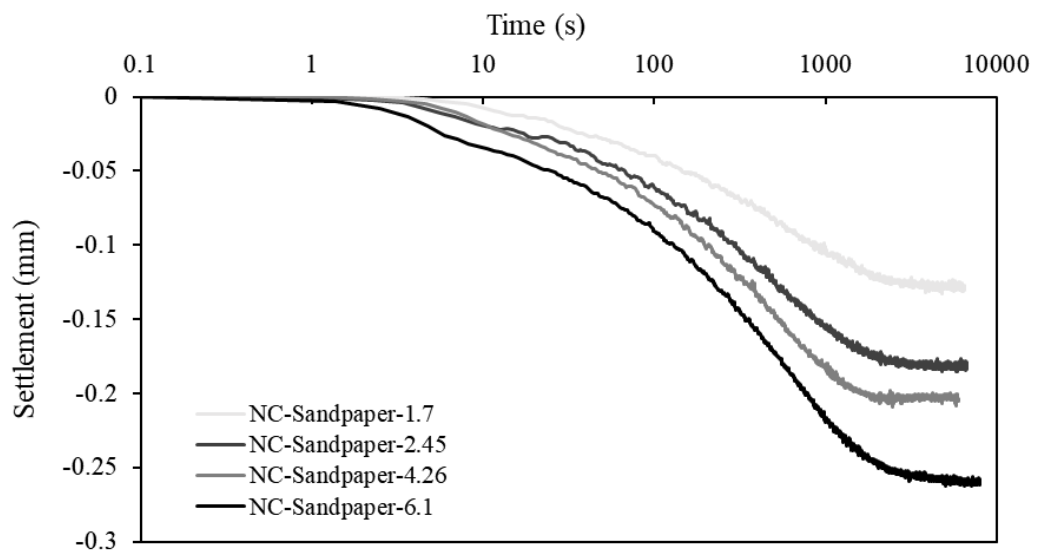


Figure 52: Consolidation of Natural Clay - Sandpaper (10mm thick specimen)

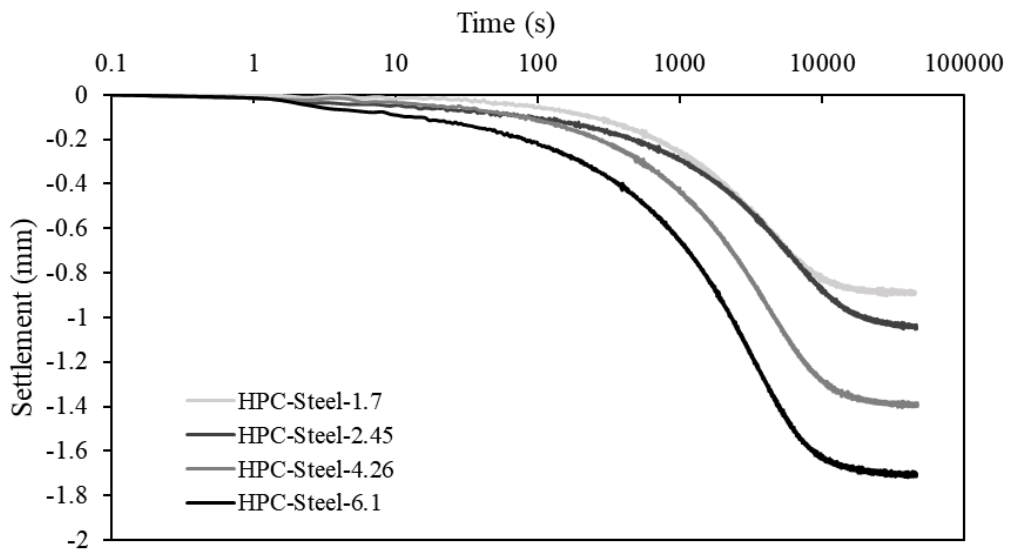


Figure 53: Consolidation of High Plasticity Clay - Stainless Steel (10mm thick specimen)

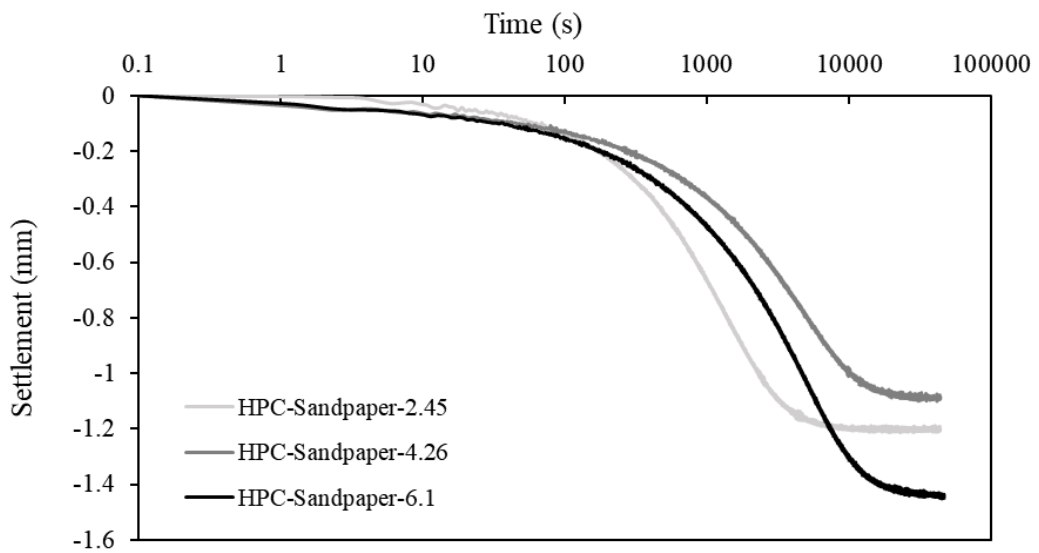


Figure 54. Consolidation of High Plasticity Clay - Sandpaper (10mm thick specimen)

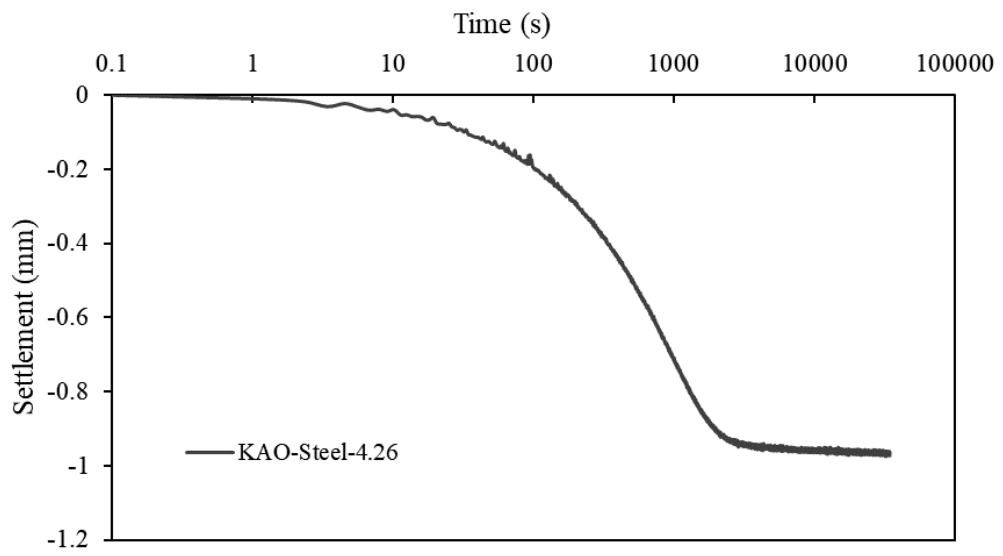


Figure 55. Consolidation of Kaolinite - Stainless Steel (10mm thick specimen)

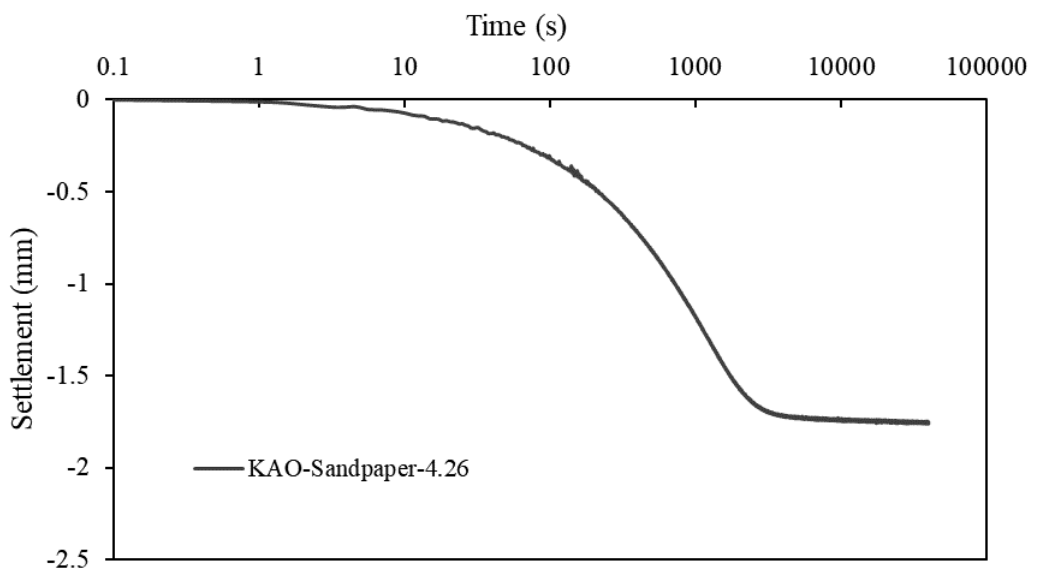


Figure 56. Consolidation of Kaolinite - Stainless Steel (10mm thick specimen)

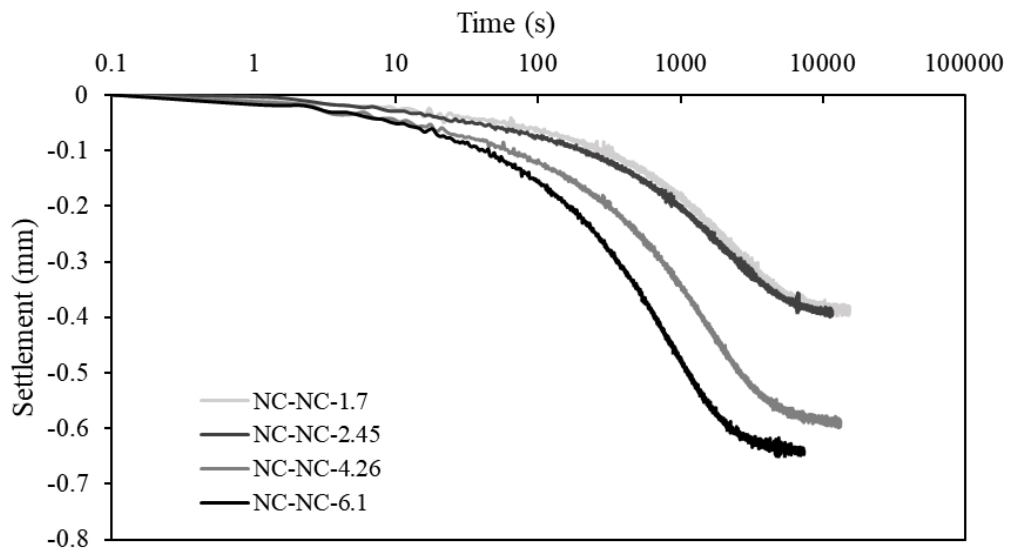


Figure 57. Consolidation of the Natural Clay (20mm thick specimen)

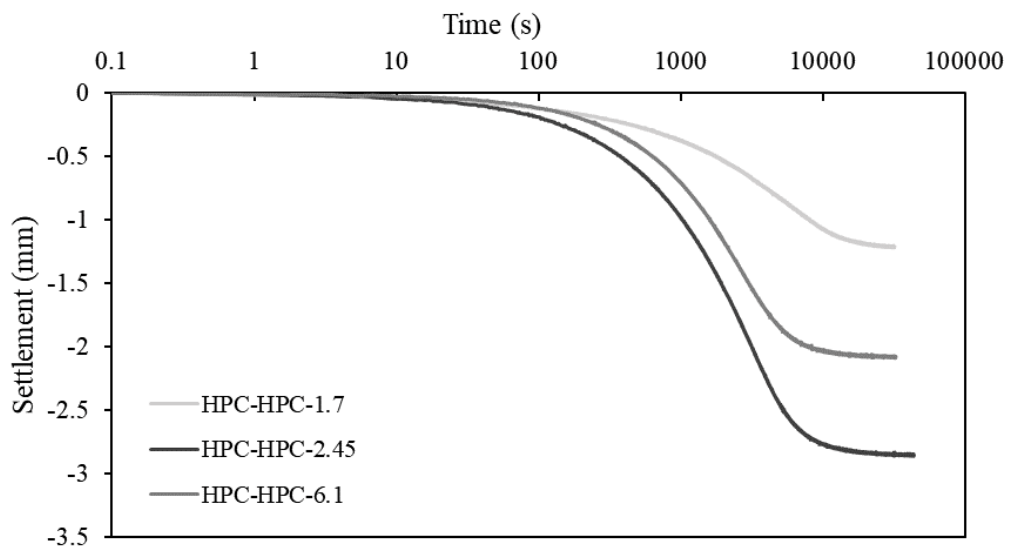


Figure 58. Consolidation of the High Plasticity Clay (20mm thick specimen)

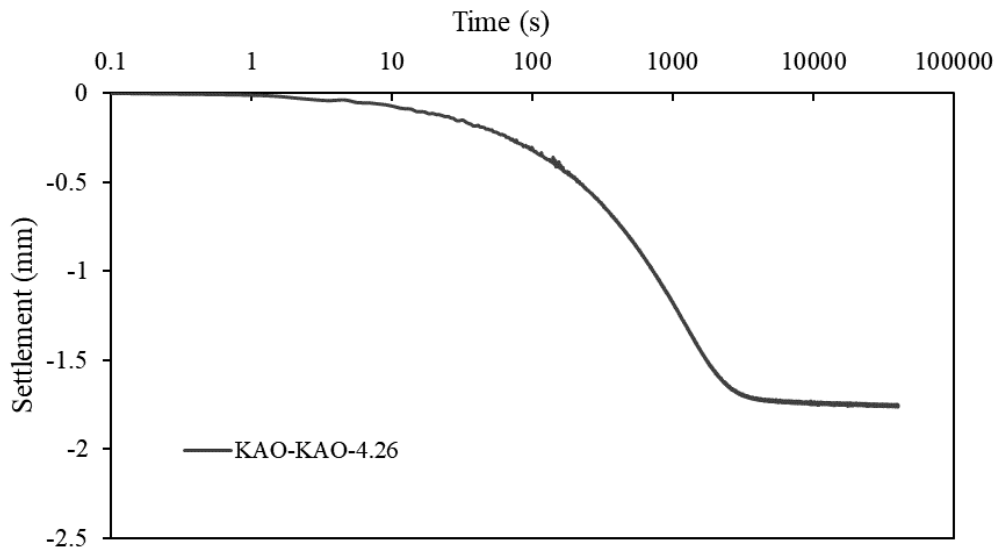


Figure 59. Consolidation of the Kaolinite (20mm thick specimen)

7.2. Peak and residual interface resistances from the Interface Direct Shear tests.

The complete interface response was captured during the interface direct shear tests. The shear stress increased until reaching a peak referred to as the peak interface resistance. Then, it decreased and plateaued, along with negligible settlements revealing that a residual resistance was mobilized. In the case of NC, reaching residual interface strength was just at after around 1mm of displacement, however, this distance increased slightly to 2-4 mm in the case of HPC, and around 5 mm when KAO was tested (Figure 63 to Figure 68). The peak resistance was mobilized under fully drained conditions as guaranteed by the adopted slow shearing rate. Accordingly, the peak and residual secant friction angles can be estimated as the arc tangent of the ratio of the shear stress to the effective normal stress at peak and large displacements, respectively. Figure 63 clearly shows this behavior for the Plexiglass interface. At a confining pressure of 4.26 kPa for example, the peak and residual shear stresses are about 1.55 and 1.3 kPa, respectively.

The corresponding secant friction angles are 20° and 17° . The corresponding peak and residual Mohr-Coulomb failure envelopes for the interface tests with Plexiglass are presented in Figure 63b. As expected, the failure envelopes are curved in the normal stress range of 1 to 6 kPa. The variation of the secant friction angle with the logarithm of the effective normal stress is shown on Figure 63d and indicates a decreasing linear variation that is consistent with the curved envelope. Note that the same behavior is observed for the other interface materials tested as shown in Figure 63 to Figure 68.

Figure 60 and Figure 61 show the failure mechanism of the HPC on the Stainless Steel and Sandpaper interfaces. A clean interface is observed when the soil slipped on the smoother Stainless-Steel interface indicating that the failure plane was along this interface. Whereas some clay particles were stuck to the Sandpaper after soil slippage revealing that probably a combined failure mechanism occurred (at the interface and at some depth within the soil). This is highly related to the interface roughness where the transition from pure interface to a within-soil failure is reported to be around $10\ \mu\text{m}$ (Tsubakihara & Kishida, 1993). The Sandpaper has a roughness R_a of around $3.5\ \mu\text{m}$ and getting an in between interface failure and shear failure in clay is somewhat expected.

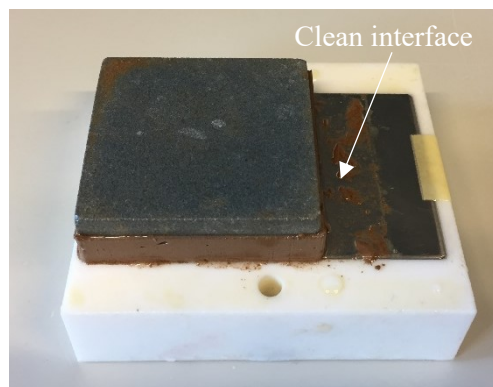


Figure 60. Failure mechanism of HPC on the Stainless Steel.

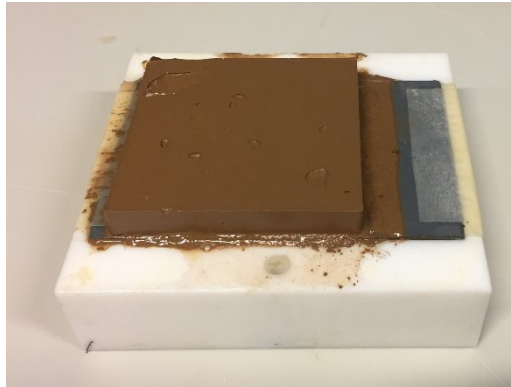


Figure 61. Failure mechanism of HPC on the Sandpaper.

In the addition to the interface direct shear tests, the three soil used in this study were tested on the same upgraded apparatus, but with replacing the lower Teflon shear box, that is designed to accept the interface material, by a conventional lower Teflon shear box designed to test and determine the internal secant friction angles of the soils at low confining pressures. The results of the tests are presented in Figure 68, Figure 69 and Figure 70, for the KAO, NC and HPC, respectively.

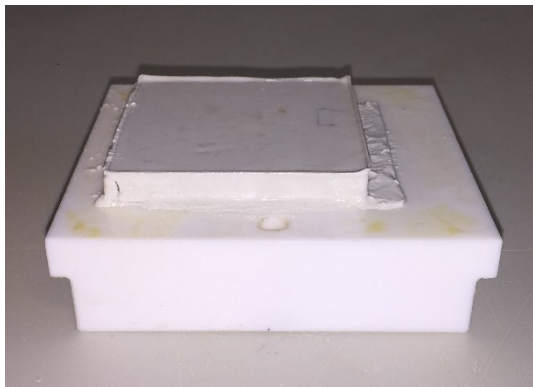


Figure 62. Direct shear test on the Kaolinite.

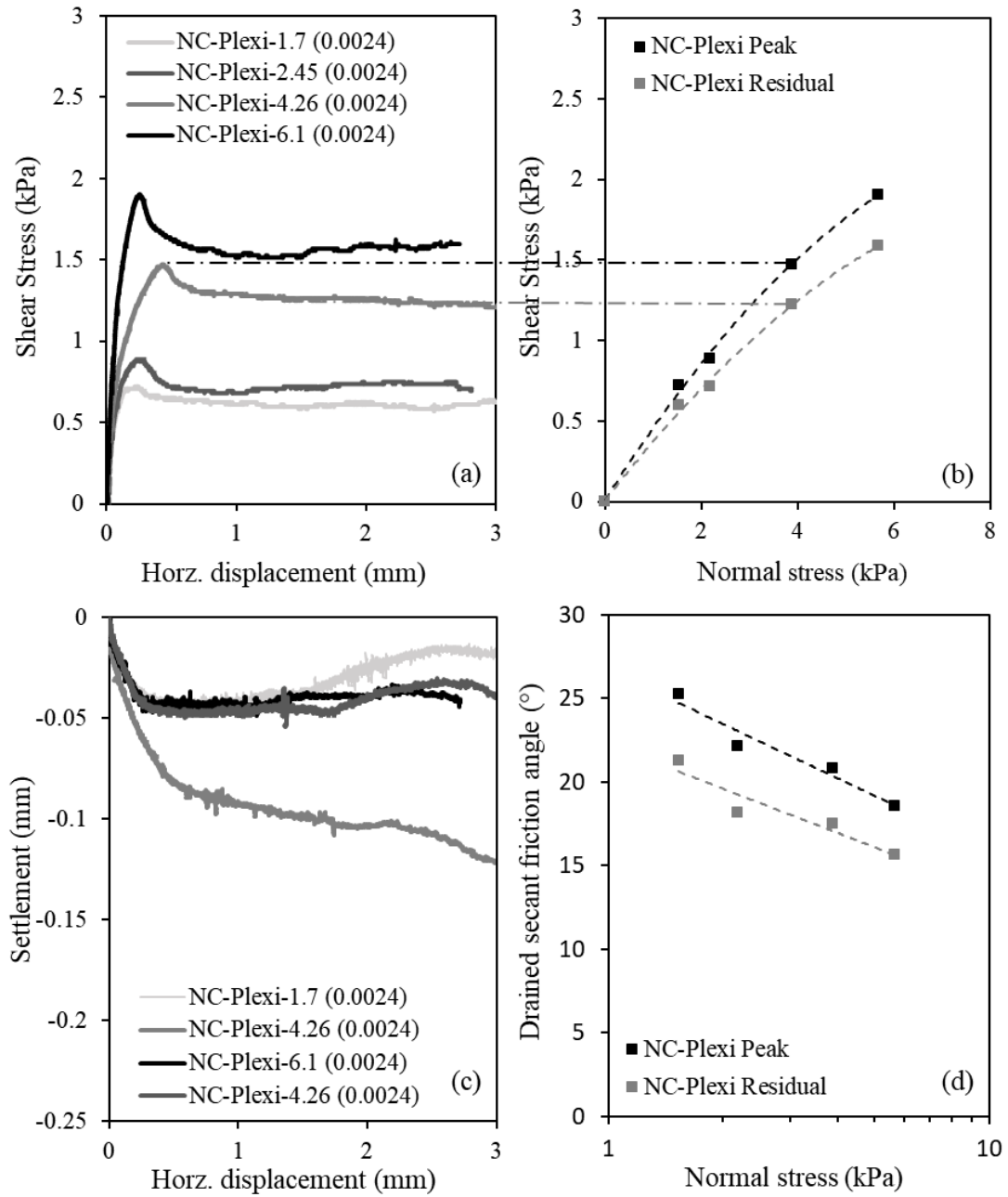


Figure 63. Interface direct shear results of NC-Plexiglass interface (a) shear stress vs displacement, (b) failure envelopes, (c) settlement during shearing, and (d) secant friction angles.

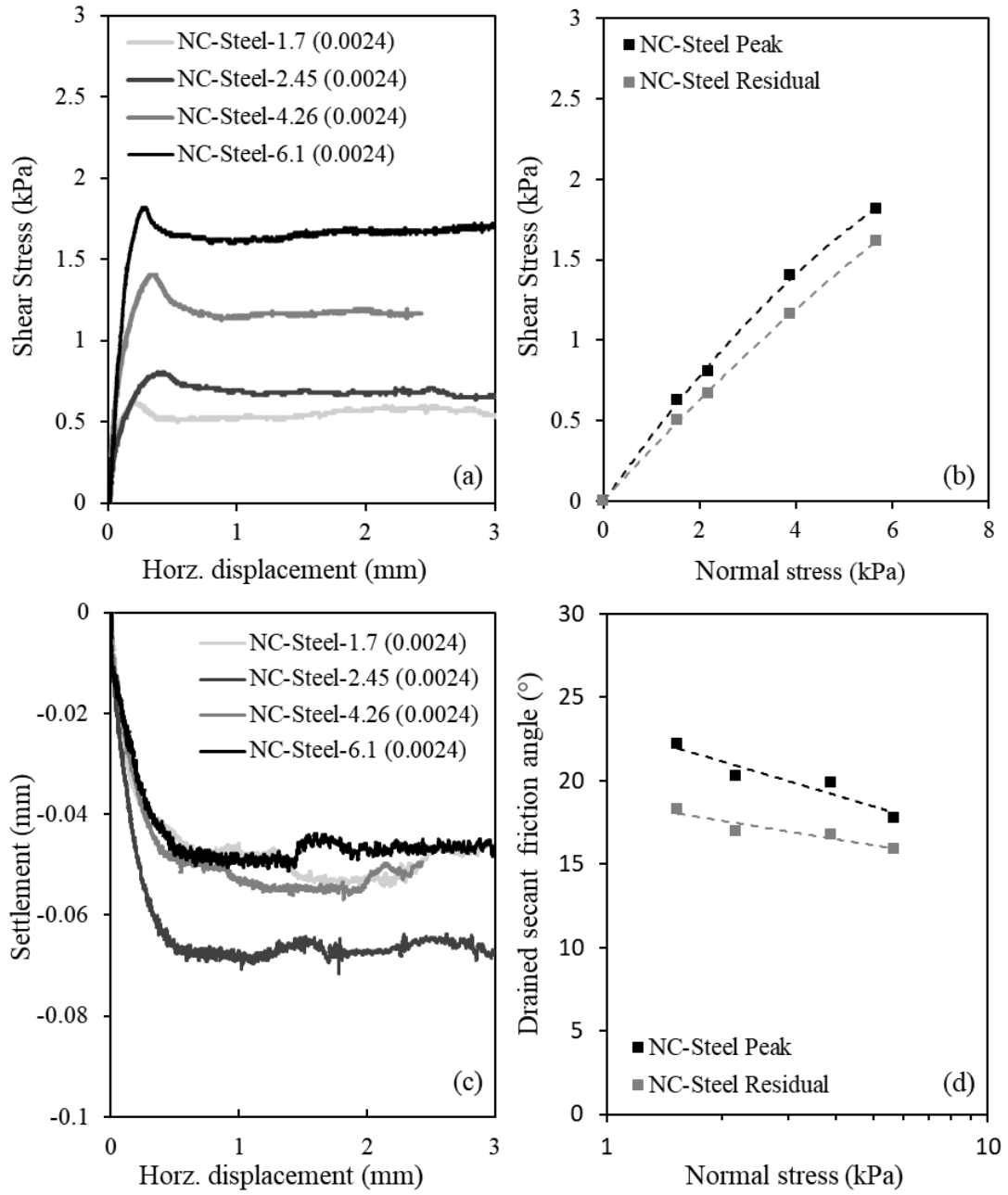


Figure 64. Interface direct shear results of NC-Steel interface (a) shear stress vs displacement, (b) failure envelopes, (c) settlement during shearing, and (d) secant friction angles.

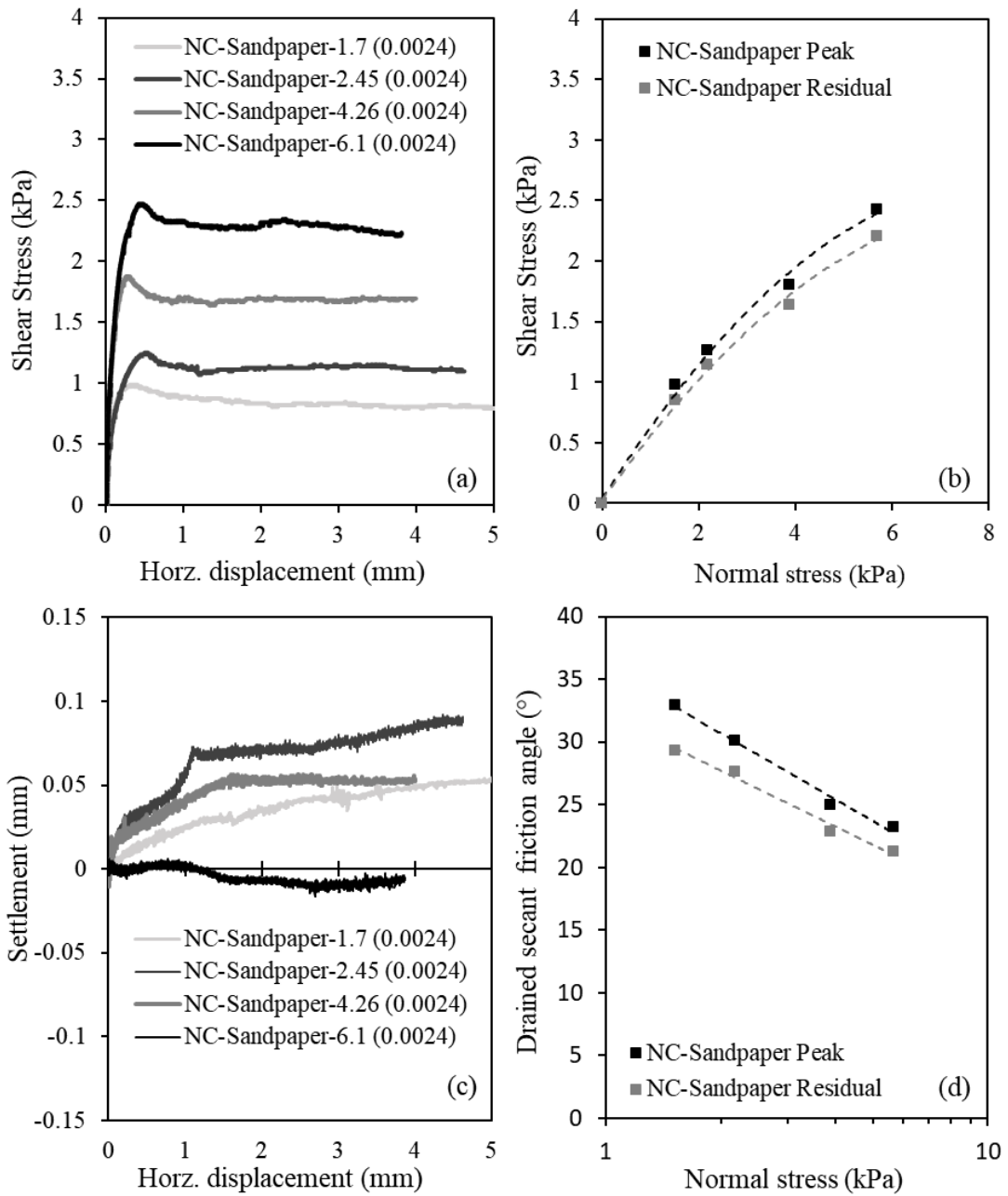


Figure 65. Interface direct shear results of NC-Sandpaper interface (a) shear stress vs displacement, (b) failure envelopes, (c) settlement during shearing, and (d) secant friction angles.

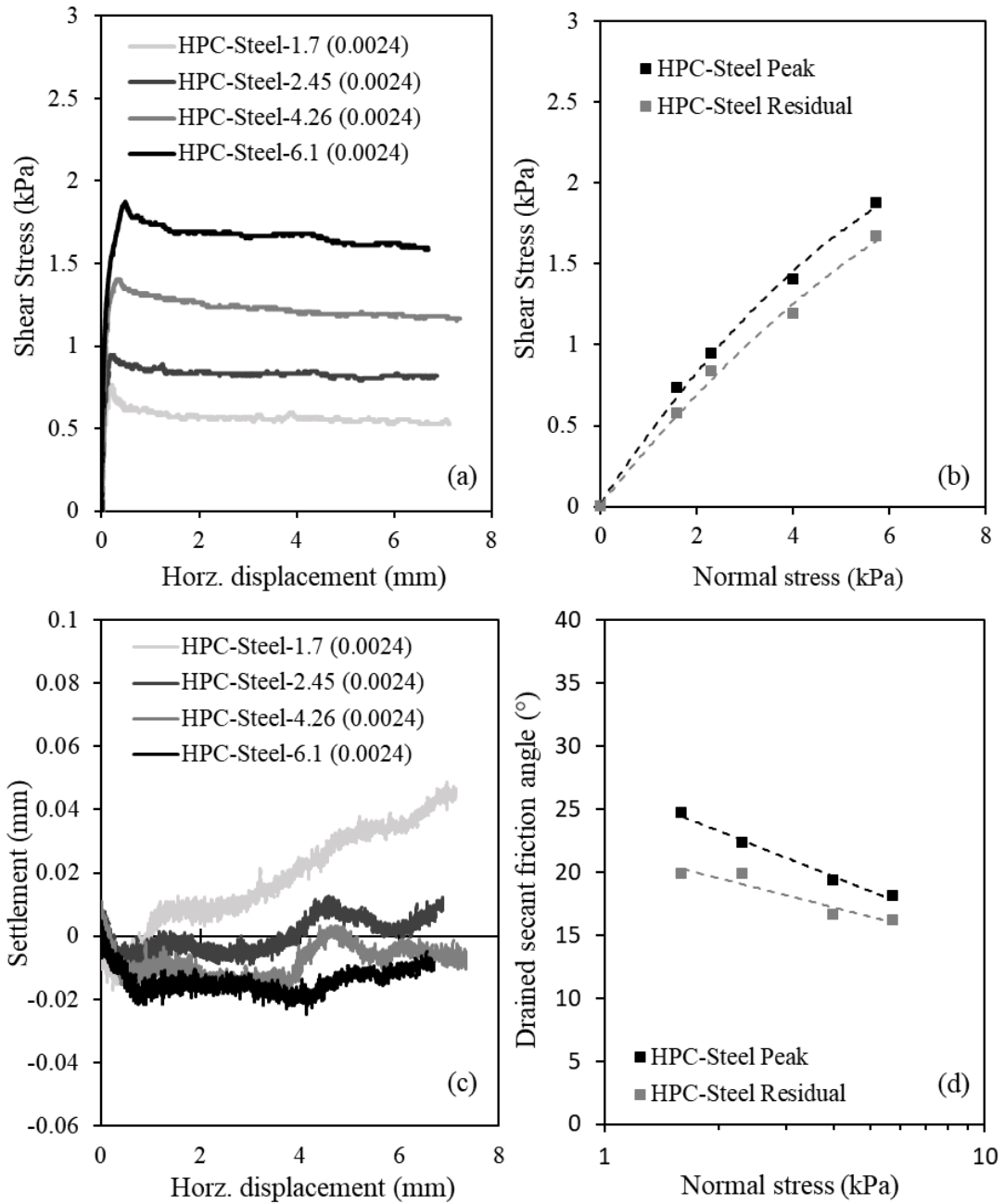


Figure 66. Interface direct shear results of HPC-Steel interface (a) shear stress vs displacement, (b) failure envelopes, (c) settlement during shearing, and (d) secant friction angles.

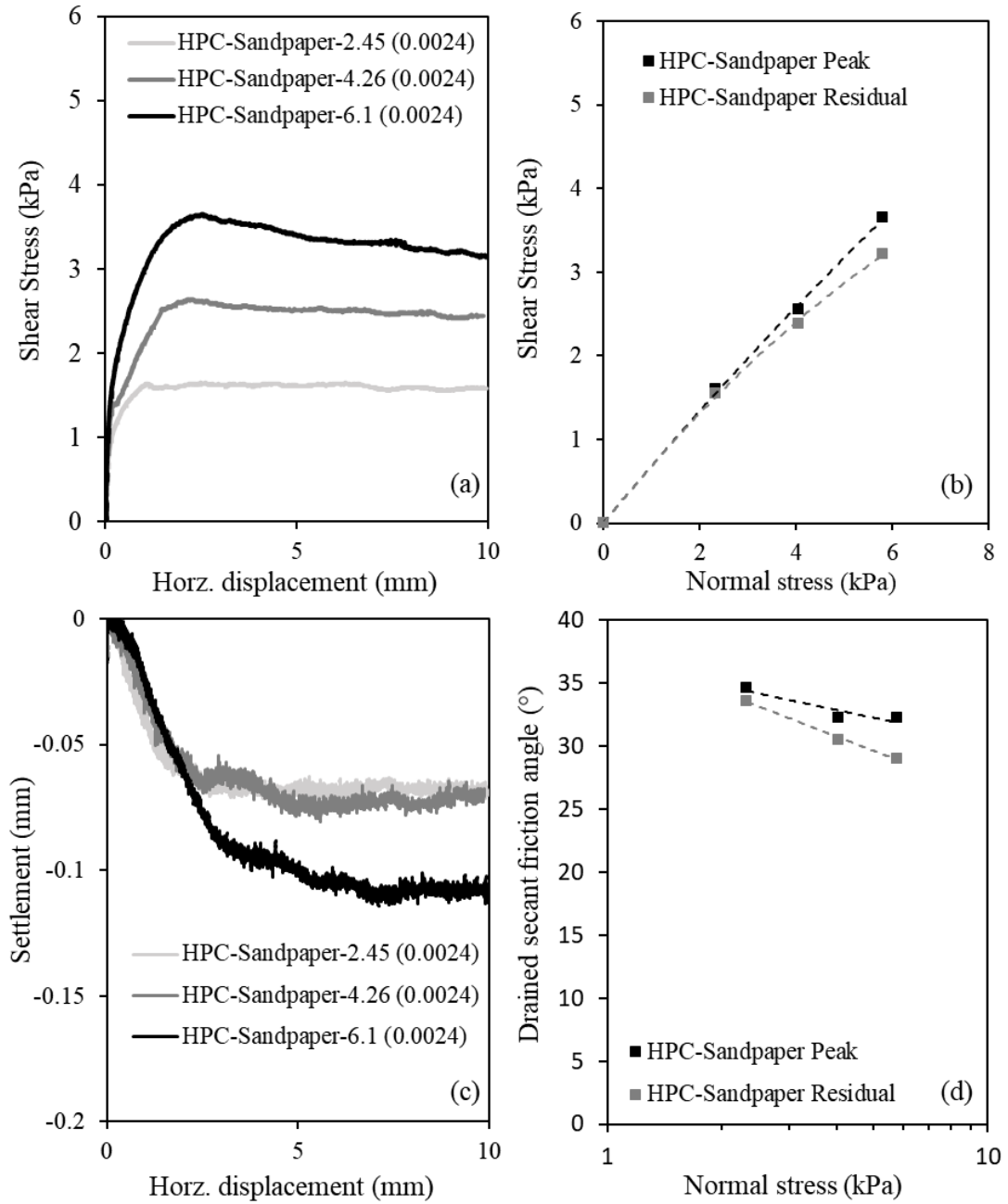


Figure 67. Interface direct shear results of HPC-Sandpaper interface (a) shear stress vs displacement, (b) failure envelopes, (c) settlement during shearing, and (d) secant friction angles.

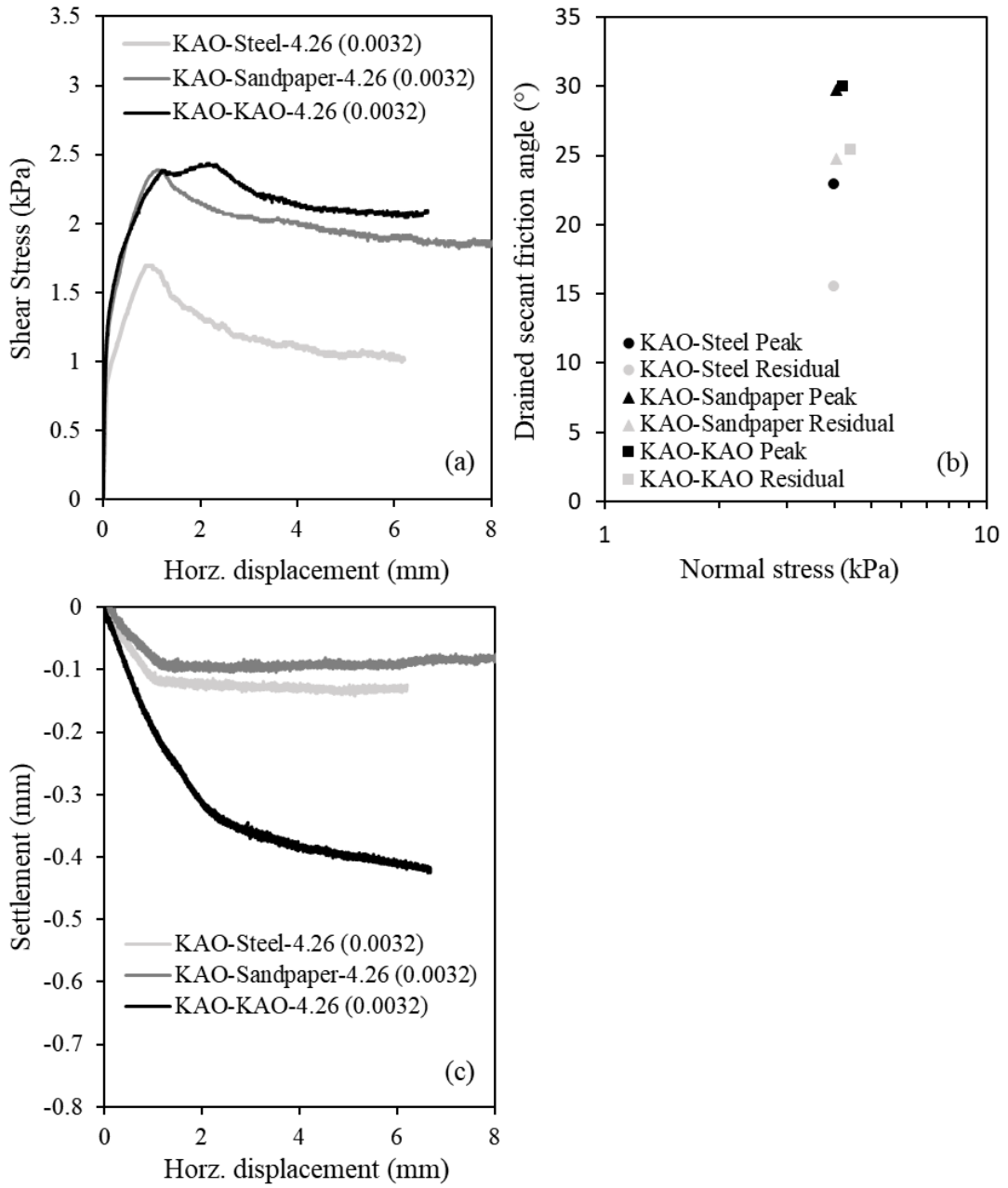


Figure 68. Direct shear tests results of the Kaolinite, and the Kaolinite on the Stainless Steel and Sandpaper: (a) shear stress vs displacement, (b) secant friction angles, and (c) settlement during shearing.

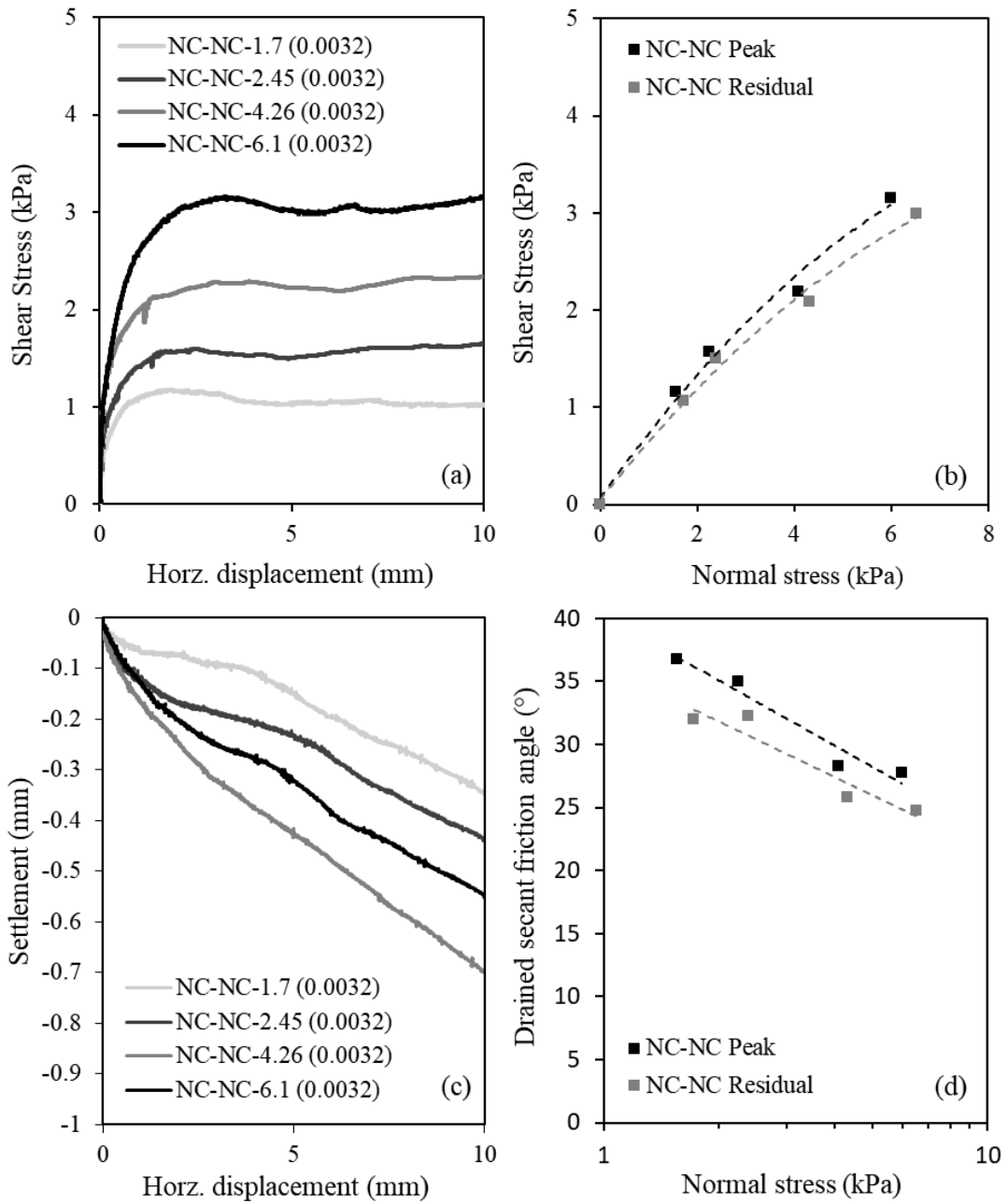


Figure 69. Direct shear tests results of NC at low normal stress (a) shear stress vs displacement, (b) failure envelopes, (c) settlement during shearing, and (d) secant friction angles.

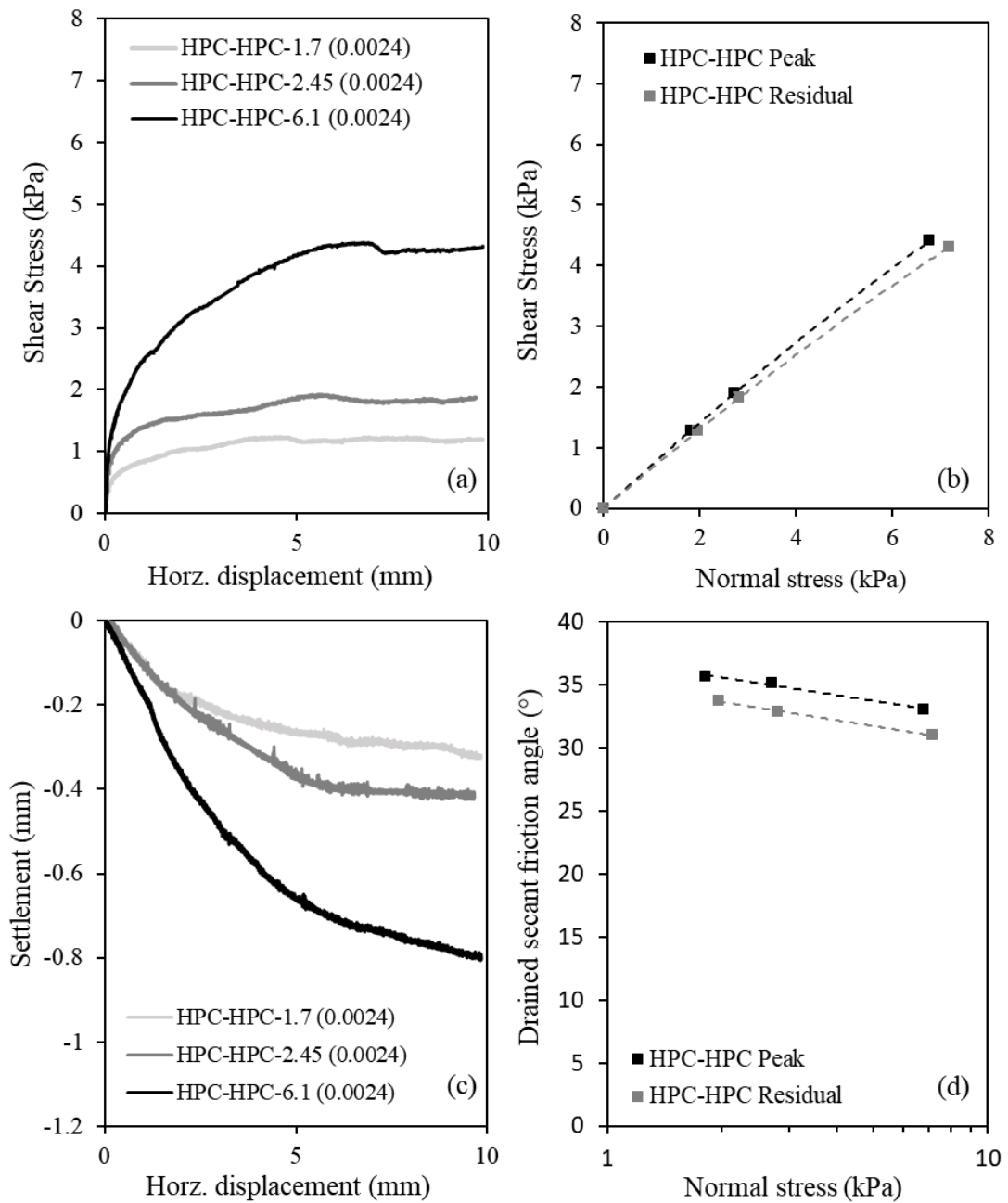


Figure 70. Direct shear tests results of HPC at low normal stress (a) shear stress vs displacement, (b) failure envelopes, (c) settlement during shearing, and (d) secant friction angles.

7.3. Residual interface resistance from tilt table tests.

Residual interface friction angles were also determined from the tilt table tests at maximum displacements in the order of 70mm. Figure 71 shows the failure mechanism of the NC (Natural Clay) on the Stainless Steel and Sandpaper interfaces. As in the case of direct shear testing, a clean interface is observed when the soil slipped on the smoother Stainless Steel interface indicating that the failure plane was along this interface. Whereas some clay particles were stuck to the Sandpaper after soil slippage revealing that probably a combined failure mechanism occurred (at the interface and at some depth within the soil).

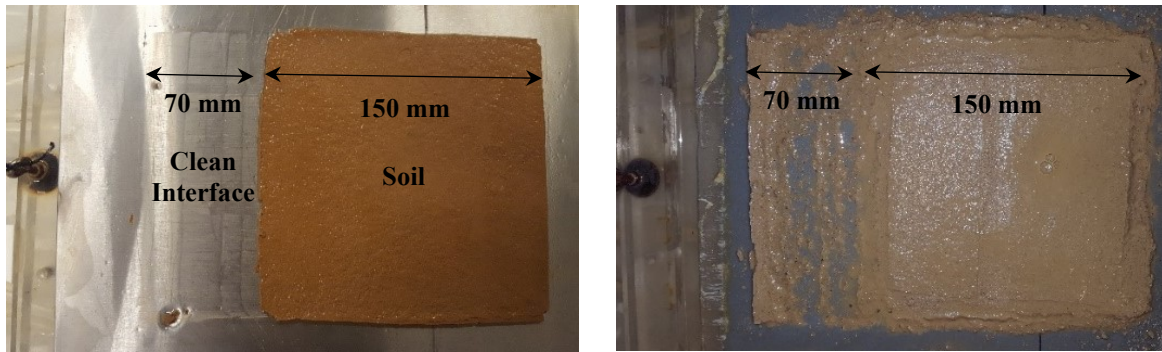


Figure 71. Failure mechanism of the natural clay on: (a) the Stainless Steel and (b) the Sandpaper

Figure 72 to Figure 77 illustrate the variation of the drained shear strength and the secant friction angle with the normal stresses for the three clays sheared against the three interface materials as obtained from the tilt table tests. Similar to the interface direct shear tests, the Mohr-Coulomb failure envelopes of the smoother interfaces (Plexiglass and Stainless Steel) were found to be curved at low normal stresses. The failure envelope of the rougher Sandpaper interface did not exhibit the same level of non-linearity with minor reductions in the secant friction angle with larger normal

stresses. Obviously, the sandpaper exhibited the highest interface resistance, where the Stainless Steel and the Plexiglass exhibited approximately similar interface responses.

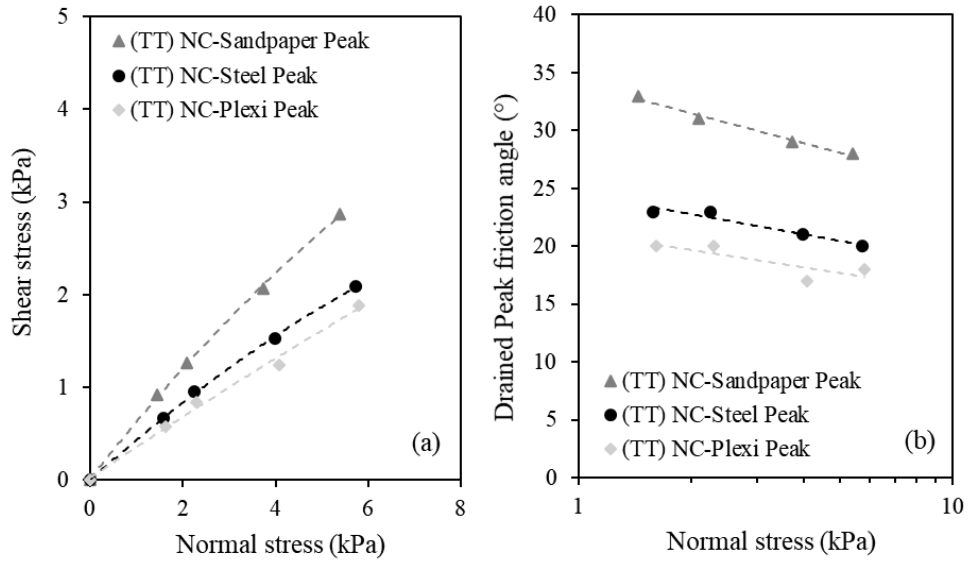


Figure 72. Variation of (a) peak interface strength and (b) peak secant friction angle with normal stresses using the tilt table (for the NC)

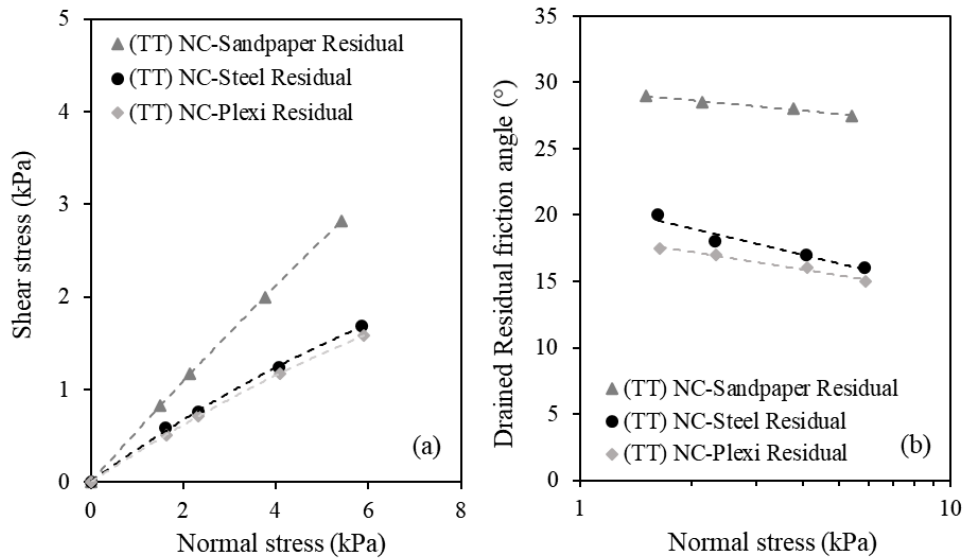


Figure 73. Variation of (a) residual interface strength and (b) residual secant friction angle with normal stresses using the tilt table (for the NC)

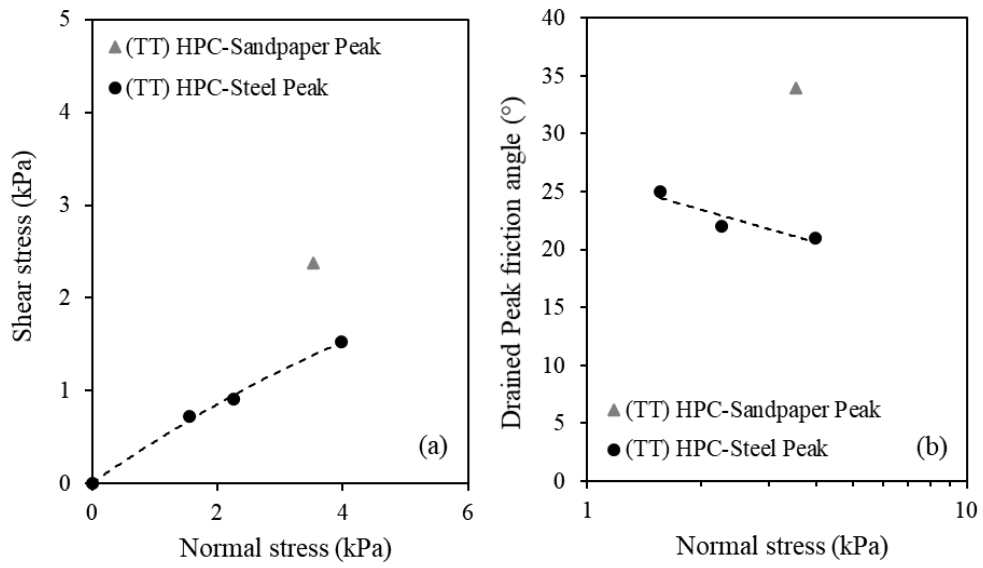


Figure 74. Variation of (a) peak interface strength and (b) peak secant friction angle with normal stresses using the tilt table (for the HPC)

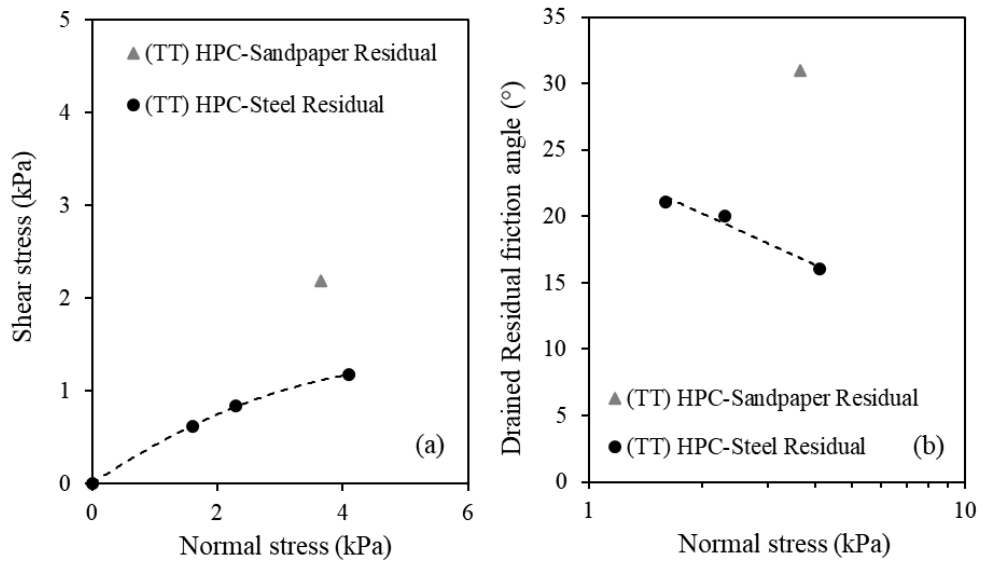


Figure 75. Variation of (a) residual interface strength and (b) residual secant friction angle with normal stresses using the tilt table (for the HPC)

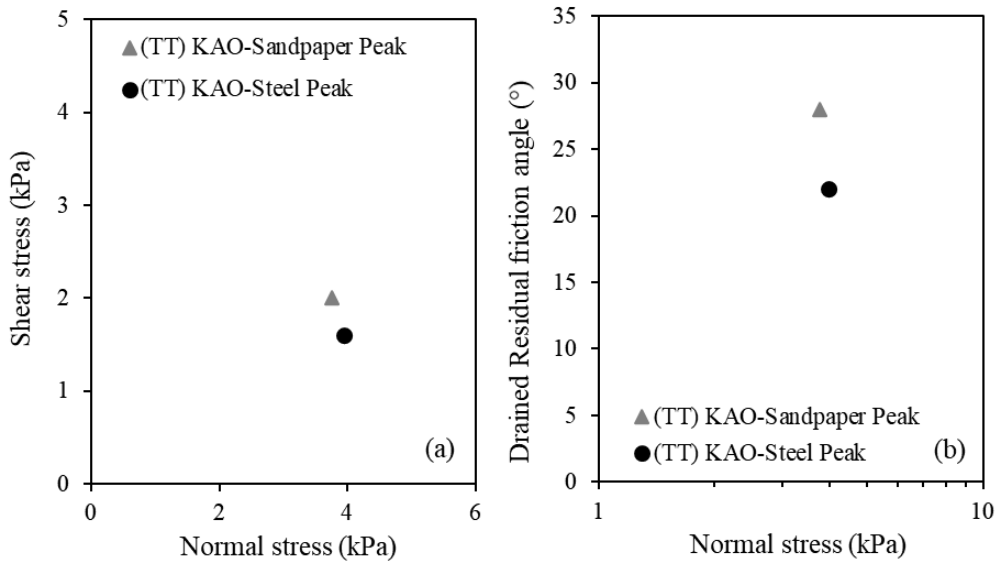


Figure 76. Variation of (a) peak interface strength and (b) peak secant friction angle with normal stresses using the tilt table (for the KAO)

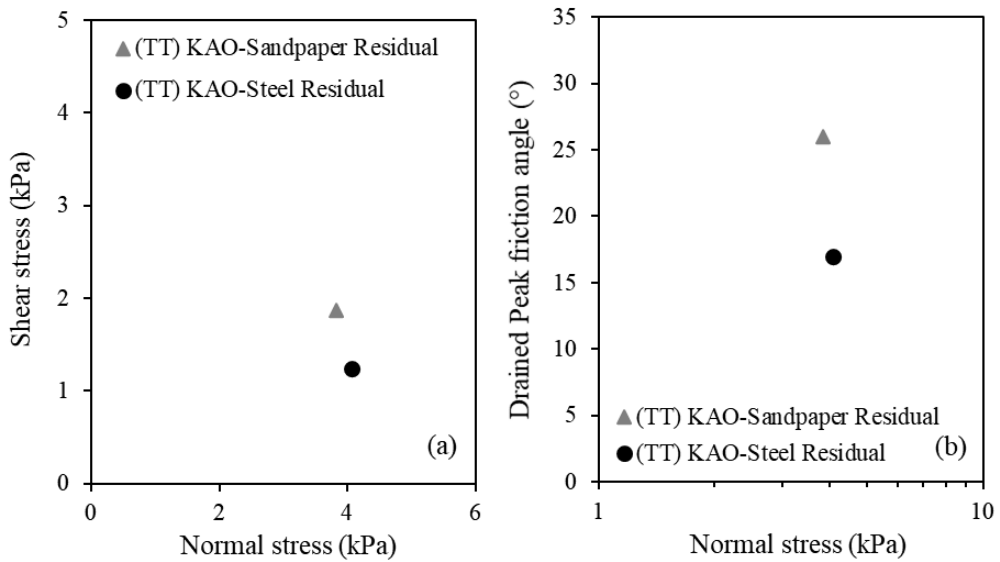


Figure 77. Variation of (a) residual interface strength and (b) residual secant friction angle with normal stresses using the tilt table (for the KAO)

7.4. Effect of roughness.

The impact of the interface roughness on the observed response can be assessed by comparing the mobilized drained interface resistance of the different interfaces either from the interface direct shear tests or the tilt table tests. Figure 78 shows the variation of the drained strength ratio ($\tan\delta_{res}$), defined as the ratio of the residual interface shear stress to the normal stress at failure, with roughness from the interface direct shear results of this study combined with the results from Westgate et al. (2018). Results indicated that increasing the roughness clearly induced an improvement in the interface strength especially in case of Sandpaper ($R_a = 3.5 \mu\text{m}$). The trends observed in Figure 78 are consistent with those reported in Westgate et al. (2018) for other interfaces.

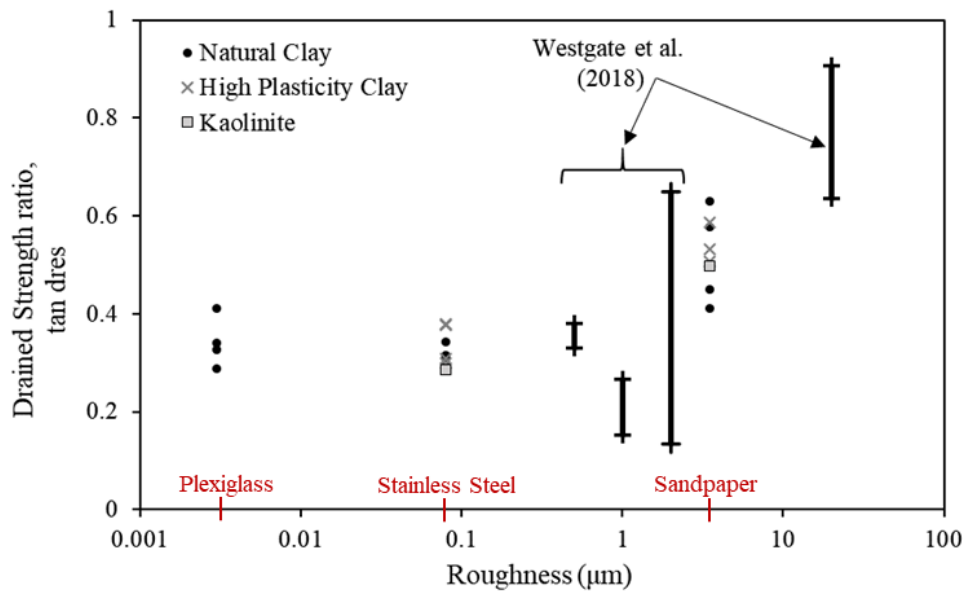


Figure 78. The variation of the drained strength ratio with the roughness on the interface direct shear testing setup.

The results of the tilt table tests were also used to calculate the interface efficiency (Equation 7) of the different interfaces used.

$$\text{Interface efficiency} = \frac{\text{Shear strength of interface}}{\text{Shear strength of soil}} \quad (7)$$

The variation of the interface efficiency with the normal stress at failure is plotted in Figure 79 for the tilt table tests that were conducted at a nominal normal stress 4.26 kPa. Results indicated that the interface is more efficient when its roughness increases. For instance, for the Natural Clay, the interface efficiency dropped from 98% for Sandpaper to 56% for the Plexiglass. It is worth noting that the Stainless Steel and Plexiglass interfaces resulted in similar coating efficiencies despite some differences in their surface roughness.

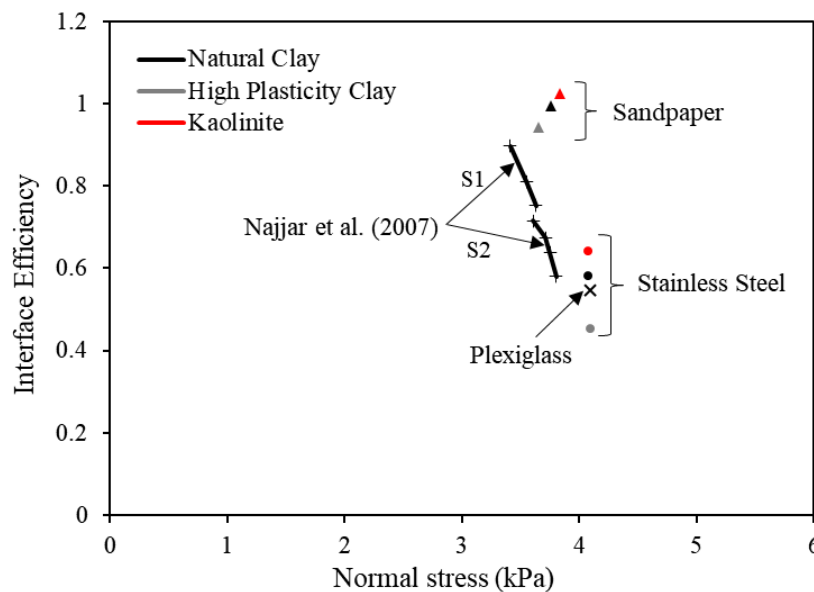


Figure 79. The variation of the interface efficiency with normal stresses on the tilt table testing setup.

7.5. Comparison between the two testing methodologies.

A direct comparison between the drained residual interface friction angles from tilt table and direct shear testing is shown in Figure 80 to Figure 82 for each soil and interface type tested in this study. Also shown on the figures are the residual friction angles of the clays as determined from the direct shear tests. Results for the smoother interfaces (Plexiglass and Steel) indicate that the two testing methodologies resulted in more-or-less similar residual secant friction angles. This observation is important since it indicates that the simple interface direct shear test setup could be used to determine the interface strength at low confining pressures provided that it is modified to eliminate mechanical friction and adapted for low pressure testing. The similarity in the residual friction angles also indicates that for the case of the remolded clay that was prepared from a slurry in this study, very small horizontal displacements (1 to 5 mm) were required in the direct shear setup to mobilize a realistic estimate of the residual friction angle. For the smooth interfaces, the only case where direct shear tests produced a notably higher residual friction angle in comparison to the tilt table was that of the Plexiglass interface at the lowest normal stress. This test will be repeated in future studies to confirm the discrepancy and attempt to explain it.

The cases with the rougher Sandpaper interface have also shown similarity between the results of tilt table and interface direct shear testing when the HPC and KAO were tested. However, in the case of NC, the Sandpaper interface indicated that the residual secant friction angles that were determined from the tilt table tests were larger than those determined from the interface direct shear tests, particularly at larger normal stresses (greater than 2 kPa). Although the two testing methodologies produced more-or-less similar residual friction angles at normal stresses less than 2 kPa

(around 27 to 29 degrees), the results of the tilt table tests did not show a steep reduction in the residual secant friction angle with normal stress as did the interface direct shear results. At the larger normal stresses, results on Figure 80c show clearly that the interface secant friction angles from the tilt table tests exceeded the internal secant friction angles of the clay itself, which is a case that is physically not admissible. One explanation for this response is that the geotextile that is under the loading plate could have interacted with the rough sandpaper interface preventing slippage of the soil on the rough interface. Such a phenomenon was observed by Najjar et al. (2007) and was solved by replacing the geotextile with a punctured geomembrane. Future work will investigate whether the relatively high interface friction angles for Sandpaper at higher normal stresses are attributed to such an interaction.

Although similarity between the two methodologies was observed for the rough interface in the case of HPC and KAO at 4.26 kPa normal stress (greater than 2 kPa where discrepancy was observed for the NC), it should be noted that the HPC and KAO were tested at one normal stress only and not several low normal stresses like in the case of NC. Further tests at several low normal stresses should be performed in the future to confirm similarity between both methodologies on the rough interface.

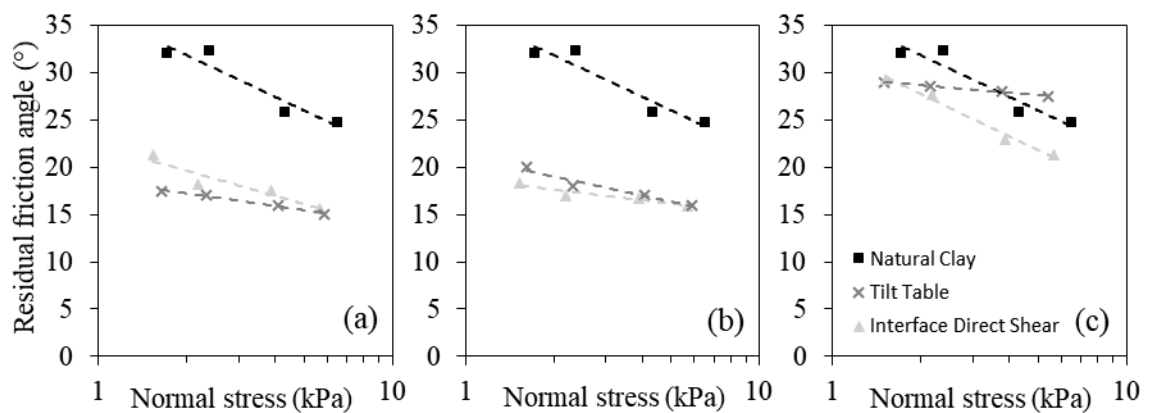


Figure 80. Residual friction angles for: (a) Plexiglass, (b) Steel and (c) Sandpaper from Tilt table and direct shear results (for the Natural Clay)

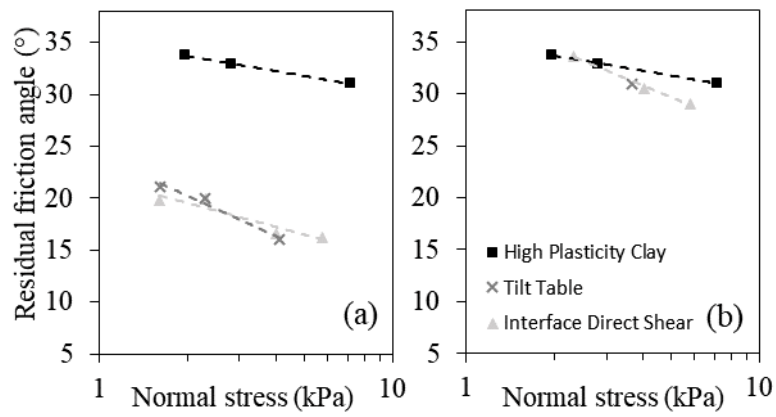


Figure 81. Residual friction angles for: (a) Steel and (b) Sandpaper from Tilt table and direct shear results (for the High Plasticity Clay)

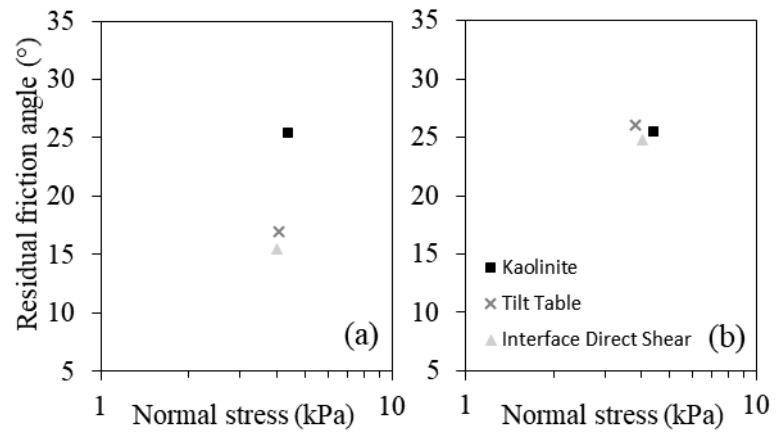


Figure 82. Residual friction angles for: (a) Steel and (b) Sandpaper from Tilt table and direct shear results (for the Kaolinite)

CHAPTER 8

CONCLUSION

The axial pipe-soil interface resistance is a key parameter in the design of HPHT pipelines. Determining it using laboratory small element testing is widely acknowledged, with the Interface Direct shear and the Tilt Table being the two most common used setups in this regard. This study aimed at comparing test results obtained using both setups with identical interfaces and soil type. The following conclusions can be drawn from a total of 45 tests performed:

- The interface friction angles obtained from both setups are relatively close for the case of smooth interfaces.
- For the case of rough interfaces, similarity was observed when the High Plasticity Clay and Kaolinite were tested under a single normal stress 4.26 kPa. However, the Interface Direct Shear appeared to give conservative results compared to the Tilt Table when the Natural Clay was tested under four normal stresses. This might have been due to a possible adverse interaction between the geotextile (under the loading plate) and the rough interface particularly at larger normal stresses. Further tests are required to confirm similarity from both setups on rough interfaces.
- The drained residual interface friction angle depends on the interface surface roughness, with recorded coating efficiency in this study ranging between 45% and 99% for the three interfaces tested.
- The Mohr-Coulomb failure envelopes for the drained residual interface resistance are curved at low confining pressure.

The comparison between both setups suggests that using the Interface Direct Shear machine for determining the drained residual pipe-soil interface resistance is a practical and reliable testing alternative, provided that the conventional direct shear setup is modified to reduce mechanical friction and make it amenable to low pressure testing.

REFERENCES

- Amarasinghe, Ruslan S., Dharma Wijewickreme, and Hisham T. Eid. 2016. "Some Observations on Soil-Pipe Interface Shear Strength in Direct Shear Under Low Effective Normal Stresses and Large Displacements." in *11th International Pipeline Conference, Calgary, Alberta, Canada, IPC2016-64100*.
- Ballard, Jean-Christophe and Richard Jewell. 2013. "Observations of Pipe-Soil Response from in-Situ Measurements." in *Proc. Of Offshore Technology Conference, 6–9 May 2013, Houston, Texas, USA, OTC 24154*.
- Boukpeti, N. and D. J. White. 2017. "Interface Shear Box Tests for Assessing Axial Pipe–Soil Resistance." *Géotechnique* 67(1):18–30.
- Boylan, N. P., D. J. White, and P. Brunning. 2014. "Seabed Friction On Carbonate Soils : Physical Modelling of Axial Pipe-Soil Friction OTC-25398-MS." in *Proc. Of Offshore Technology Conference, 5–8 May 2014, Houston, Texas, U.S.A, OTC-25398-MS*.
- De Brier, Charles, Jean-Christophe Ballard, and David Colliard. 2016. "On the Added Value of Advanced Interface Shear Testing for Pipeline Walking Mitigation." Pp. 1–15 in *Proc. Offshore Pipeline Technology Conf. Amsterdam, Feb. 24-25*.
- Dunlop, D. G., N. T. Brewster, S. P. G. Madabhushi, A. S. Usmani, P. Pankaj, and C. R. Howie. 2000. "Mechanical Strength of Impaction Bone Grafting—The Effect of Washing the Graft." *J. Bone Jt. Surg.* 85:639–646.
- Eid, Hisham T., Ruslan S. Amarasinghe, Khaled H. Rabie, and Dharma Wijewickreme. 2014. "Residual Shear Strength of Fine-Grained Soils and Soil–Solid Interfaces at Low Effective Normal Stresses." *Canadian Geotechnical Journal* 52(2):198–210.
- Ganesan, S., M. Kuo, and M. Bolton. 2014. "Influences on Pipeline Interface Friction

- Measured in Direct Shear Tests.” *ASTM Geotechnical Testing Journal* 37(1):94–106.
- Ganesan, Senthil, Matthew Kuo, and Malcolm Bolton. 2014. “Geotechnical Testing Journal Influences on Pipeline Interface Friction Measured in Direct Shear Tests Influences on Pipeline Interface Friction Measured in Direct Shear Tests.” *Geotechnical Testing Journal* 37(1):1–13.
- Haustermans, L. A. G. 2002. “Effect of Coating on Resistance to Movement of Pipelines on Clay Seabed.” *MPhil Thesis, University of Cambridge, Cambridge, UK*.
- Hill, AJ, DJ White, DAS Bruton, T. Langford, V. Meyer, R. Jewell, and J. C. Ballard. 2012. “A NEW FRAMEWORK FOR AXIAL PIPE-SOIL RESISTANCE , ILLUSTRATED BY A RANGE OF MARINE CLAY DATASETS.” *Proc. 8th Int. Conf. on Offshore Site Investigation and Geotechnics. SUT, London. (January)*.
- Hill, Andrew John and Helene Jacob. 2008. “In-Situ Measurement of Pipe-Soil Interaction in Deep Water.” in *Proc. Of Offshore Technology Conference, 5–8 May 2008, Houston, Texas, U.S.A, OTC 19528*.
- Kuo, M. Y. H., C. M. Vincent, M. D. Bolton, A. J. Hill, and M. Rattley. 2015. “A New Torsional Shear Device for Pipeline Interface Shear Testing.” Pp. 405–10 in *Proc. 3rd International Symposium Frontiers in Offshore Geotechnics, Oslo*.
- Low, HE, M. Ramm, MF Bransby, DJ White, and Zj Westgate. 2017. “Effect of Through-Life Changes in Soil Strength and Axial Pipe-Seabed Resistance for HPHT Pipeline Design.” Pp. 841–49 in *Proc. Int. Conf. on Offshore Site Investigation and Geotechnics. SUT, London. Vol. 675*.
- Najjar, S. S., R. B. Gilbert, E. Liedtke, B. McCarron, and A. G. Young. 2007. “Residual

- Shear Strength for Interfaces between Pipelines and Clays at Low Effective Normal Stresses.” *Journal of Geotechnical and Geoenvironmental Engineering* 133(6):695–706.
- Najjar, Shadi S., Robert B. Gilbert, Cockrell Hall, and Bill Mccarron. 2003. “Omae2003- 37499.” 1–8.
- Pedersen, Robert C., Roy E. Olson, and Alan F. Rauch. 2003. “Shear and Interface Strength of Clay at Very Low Effective Stress.” *Geotechnical Testing Journal* 26(1):71–78.
- Randolph, M. F., D. J. White, and Y. Yan. 2012. “Modelling the Axial Soil Resistance on Deep-Water Pipelines.” *Géotechnique* 62(9):837–46.
- Senthilkumar, M., J. Kodikara, P. Rajeev, and D. J. Robert. 2013. “Axial Pipe-Soil Interaction Behaviour of Offshore Pipelines.” *Australian Geomechanics Journal* 48(4):123–36.
- Senthilkumar, M., P. Rajeev, J. Kodikara, and N. I. Thusynathan. 2011. “Laboratory Modelling of Pipe-Clay Seabed Interaction in Axial Direction.” Pp. 95–102 in *Proc. 21st International Offshore and Polar Engineering Conference*. Vol. 8.
- Smith, V. B. and D. J. White. 2014. “Volumetric Hardening in Axial Pipe Soil Interaction.” in *Proc. Of Offshore Technology Conference Asia, 25–28 March 2014, Kuala Lumpur, Malaysia, OTC-24856-MS*.
- Stanier, S. A., D. J. White, S. Chatterjee, P. Brunning, and M. F. Randolph. 2015. “A Tool for ROV-Based Seabed Friction Measurement.” *Applied Ocean Research* 50:155–62.
- Stark, T. D. and H. T. Eid. 1993. “Modified Bromhead Ring Shear Apparatus.” *Geotechnical Testing Journal, ASTM* 16(1):100–107.

- Westgate, Z. J., D. J. White, and M. Savazzi. 2018. "Experience with Interface Shear Box Testing for Axial Pipe-Soil Interaction Assessment on Soft Clay." in *Proc. Of Offshore Technology Conference, 30 April - 3 May 2011, Houston, Texas, Usa, OTC-28671-MS*.
- White, D., A. Hill, Z. Westgate, and J. C. Ballard. 2010. "Observations of Pipe-Soil Response from the First Deep Water Deployment of the SMARTPIPE®." *Frontiers in Offshore Geotechnics II* (October):851–56.
- White, D. J., M. E. Campbell, N. P. Boylan, and M. F. Bransby. 2012. "A NEW FRAMEWORK FOR AXIAL PIPE-SOIL INTERACTION , ILLUSTRATED BY SHEAR BOX TESTS ON CARBONATE SOILS." in *Proc. 8th Int. Conf. on Offshore Site Investigation and Geotechnics. SUT, London*.
- White, D. J., S. A. Ganesan, M. D. Bolton, D. A. S. Bruton, J. C. Ballard, and T. Langford. 2011. "SAFEBUCK JIP - Observations of Axial Pipe-Soil Interaction from Testing on Soft Natural Clays." in *Proc. Of Offshore Technology Conference, 2–5 May 2011, Houston, Texas, Usa, OTC 21249*.
- White, David J. and Mark Randolph. 2007. "Seabed Characterisation And Models For Pipeline-Soil Interaction." *Journal of Offshore and Polar Engineering* 17(3):193–204.
- Wijewickreme, Dharma, Ruslan Amarasinghe, and Hisham Eid. 2014. "Macro-Scale Direct Shear Test Device for Assessing Soil-Solid Interface Friction under Low Effective Normal Stresses." *Geotechnical Testing Journal* 37(1).